UNIVERSITY OF ARKANSAS
GRADUATE INSTITUTE OF TECHNOLOGY

TECHNOLOGY CAMPUS
1201 McALMONT
LITTLE ROCK, ARKANSAS

October 11, 1965

Dr. T. L. K. Smull, Director
Grants and Research Contracts Division
Office of Space Science and Applications
Code SC
National Aeronautics and Space Administration
Washington, D. C. 20546

Dear Dr. Smull:

This letter and the attached individual project progress reports constitute the semiannual status report on the research work supported by NASA under Research Grant NsG 713 to the University of Arkansas entitled "Investigation of Laser Properties Relevent to the Measurement of Different Physical Parameters" for the period March 1, 1965 through September 1, 1965.

In general the above period of time was involved in determining theoretically and experimentally the feasibility of several original ideas. Some of the ideas still appear to be feasible while others have been rejected after their investigation. A list of the projects, which have been divided into present investigations, temporarily suspended projects, and cancelled projects, can be found in the Table of Contents following this letter.

Listed below are several ideas that have been advanced for future evaluation relative to the feasibility of using the various types of lasers as an integral part of a system. To qualify for investigation or experimentation, the system must utilize the laser in a unique manner, improve accuracy or sensitivity over existing devices, or allow simplification of the device or its auxiliary equipment. It should be noted that no theoretical or experimental evaluation has been performed to date on the ideas presented below.

FUTURE WORK

1. Surface Smoothness Guage

This proposed device would utilize a laser beam directed normal to the surface to be measured. If a uniform reflecting surface is moved perpendicularly through a laser beam, the irregularities of the surface would give rise to a variation in the nature of the reflected and scattered radiation. In other words, the irregularities will present surfaces advancing toward and receding from the beam, given rise to Doppler shifts.

If the reflected radiation is then heterodyned with the incident radiation, the resulting signal would possibly give an indication of the distribution of the sizes and types of the irregularities by means of a spectrum analyzer measuring the power spectrum of the heterodyned signal. The feasibility of this device could be determined from a detailed theoretical analysis of the signal detection problem.

2. Hologram Schlieren Photography

A proposed area of investigation is the use of holograms in making schlieren photographs. One should be able to make a number of reconstructions of the same hologram using different sensitivities. In addition to this, the "lensless photography" aspects of holography might be utilized to escape the present field size limitation imposed by mirror size.

3. Laser Interferograms

A second use of lasers in studying small density variations might be through simplification of the making of interferograms. One might be able to use moire fringes in viewing these interferograms.

4. Orientation of a Corner-Cube Reflector

It is anticipated that a study will be made as to the feasibility of a proposed method for determining the orientation of a distant corner-cube reflector.

5. Moire Mapping of Opaque Surfaces

Another proposed area for future work is the use of lasers to form interference fringes on the surface of opaque objects. The observer would then view these fringes through a grating and use the resultant moire fringes in mapping the surface.

6. A Method of Measuring the Angular Velocity and/or Acceleration of a Rotating Device Such as an Ultra-centrifuge

A device of this type might be used where surface requirements of the rotating equipment will not allow markings of any type on the surface. The velocity would be measured by taking the light scattered in the direction of rotation and the light scattered in the opposite direction, mixing the two scattered radiations together and obtaining a double Doppler frequency shift.

Sincerely yours,

M K Testerman

M. K. Testerman
Principal Investigator

MKT/ac

TABLE OF CONTENTS

Present Investigations

Temporarily Suspended Projects

Cancelled Projects

Illustrations

LIST OF FIGURES

PRESENT INVESTIGATIONS

MAPPING OF VIBRATING SURFACES

C. Young

Introduction

This project involves the mapping of vibrating surfaces by using the laser Doppler and Interference fringe techniques. These techniques are ideally suited for such a process and a study has been initiated to determine their feasibility. It is possible to develop techniques that would determine resonant frequencies and modes of vibration in panels and other surfaces. Membranes and diaphragms of various shapes and depth could be analyzed and compared to theoretical models. Figure 1 illustrates several common modes of circular and rectangular membranes not bounded at the center, and it also shows some of the equations involved with in this study. The theory on these forms is established, and these forms can be used as models for study and development. Similar functions are characteristic for rectangular bounded surfaces. A level of confidence in these techniques could be achieved from the verification of the experimental mapping with theoretical analysis of the various modes of vibration. Then measurement of shapes and conditions that have theoretically and mathematically been difficult could be studied. This method of vibration analysis is a non-destructive type of testing and is completely isolated from the system parameters under measurement. This system, in a unique sense, performs as a mapping radar which is capable of measuring displacement, velocity and acceleration in one operation.

Work Performed

Data from the membrane used in the study involving pressure transducers was analyzed. Resonant fundamental frequency techniques were established and higher

vibrations of the membrane were observed superimposed on the fundamental. From the Bessels functions of the zero order the following frequency relationships indicate the possibility of the fourth mode as the first near harmonic following the fundamental.

Fundamental .....

Second mode ..... 2.3 (fundamental)

Third mode ..... 3.5 (fundamental)

Fourth mode ..... 4.9 (fundamental)

(approximately the fifth harmonic)

Information such as acceleration, peak velocity and displacement was determined as a function of time.

At present, the Doppler data varies both in amplitude and frequency, although the amplitude variations are meaningless for readout. Logarithmic compressional amplifier techniques are being studied to provide constant amplitude for varying inputs so that frequency dependent voltages can be developed. The frequency dependent voltage will provide graphic velocity and acceleration data. The graphic amplitude is analogous to the velocity, the slope, and the acceleration.

There were three methods for gathering data: a point by point mapping system and two synchronous timing methods, one involving a gas laser and the other a pulsed laser. The point by point mapping system provided all the vibrational information at one point, and a read out of the points provided mode functions and maximum vibrational displacement over any area. A functional schematic diagram of this point by point mapping system is shown in Fig 2.

A second method of gathering data from a vibrating surface consisted of a synchronous timing method, in which the vibration was stopped at a unique position and the interference pattern was read out for that particular instantaneous position

of the surface. Pulse modulation of the laser was required for proper illumination timing.

The purpose of providing synchronous presentation was to supply total area photographs showing modes, displacement and shape at any instant of time from one piece of data. This mapping technique can supply a large amount of data in a short time and may be more efficient and as equally effective as point by point mapping for some special surfaces. Preliminary work has been done in this area. Since fringe patterns obviously become dense across the gradients for extremely large vibrations, this method will perhaps be more useful in areas and surfaces of small vibrations such as one would normally study in a laboratory. Figure 3 is a functional diagram showing a synchronous system using a gas laser. The laser illuminated a surface only at a chosen vibrational position, and the film was exposed long enough to record the interference pattern of that position.

The basic problem in this system was to eliminate undesired interference patterns caused by the surfaces of plates in the optics system and pulse modulation of the laser. The synchronous relationships were obtained with standard, off the shelf test equipment. The frequency generator was the timing control for the entire system and fixed delays were handled in the pulser. Since pulsing of the laser at a high rate and a short pulse width might have been a limiting factor, another synchronous method was considered. This method consisted of chopping the laser beam at a synchronized rate or at a slightly different frequency. When the vibration was set at a rate of 500 times/sec and the chopper rate 501 times/sec, the surface fringe pattern shrank and increased twice each second. This rate of change, in which the normal continuous illumination expansion and contraction rate was 1000 times/sec, was observable with the unaided eye. For a particular point, a coincidence timing relationship was derived from this system, in which once every second, at the same vibrational position, the surface was

illuminated with collimated laser light and the fringes were integrated on an exposed photographic plate. This situation was essentially the same in which the fringe patterns were at a frozen position to be examined. The main problems with this method were the amount of light available and timing and coincidence circuitry, most of which has already been basically established. The chopper was driven by a variable speed synchronous motor and its velocity was monitored by various easily achieved methods. Figure 4 is a timing synchrogram of the above arrangement.

The third method, also a synchronous timing system, involved the use of a pulsed laser instead of a gas laser. The advantages of this type of laser were that integration of the signal over a period of time was not necessary, and the energy from one pulse of the laser was sufficient to be recorded on a photographic film. The disadvantage was the lack of certainty of alignment until after attempts at recording data had been made. If, however, such a system could be made stable enough for portable use, or were to be used constantly in the same position, alignment would only have to be adjusted periodically or when data was not being satisfactorily recorded. A study of available energy and film speeds needs to be made for feasible parameters prior to the implementation of hardware for this method.

Future Work

The laboratory at GIT is well supplied with the equipment necessary to launch the above study. The first two methods of observing the vibrations with lasers have already shown considerable promise and progress is being made. Graphical data of several surfaces will soon be plotted as a system, as has been done manually in the preliminary study. It is believed that, as a result of the techniques developed within this study, little effort would have to be added to

provide a field usable instrument for vibrational data. Further and more intimately detailed knowledge of vibrations should be obtainable by these methods and develop into a useful study.

THE USE OF A LASER TO MEASURE THE FREQUENCY RESPONSE OF A TRANSDUCER

T. W. Martin

Introduction

The work conducted on the momentum detector described in a previous report resulted in the application of the laser beam to the observation of vibrating surfaces such as measuring the frequency response of a microphone. This new application appears attractive since it does not depend upon the transmission of sound or resonant cavities and it imposes no additional load on the device being tested. This method is capable of a frequency response comparable to any microphone and it may be used to observe surfaces in a vacuum where there is no loading because of the atmosphere.

Work Performed

This investigation was based on the theory of a laser feedback system in which the laser beam was reflected from the vibrating microphone, through the laser and into a photomultiplier tube as shown in Fig 5. The output from the photomultiplier tube was observed on an oscilloscope. The reflected beam from the vibrating membrane produced Doppler fringes which appeared at the photomultiplier surface. One fringe was produced for each half wavelength of the incident radiation traveled by the diaphragm toward or away from the laser. As the diaphragm moved through the center or relaxed position, the fringes were produced at the maximum rate because of the high velocity of the diaphragm at that position. As the diaphragm came to rest at the maximum deflection, the fringe rate approached zero. This change in fringe rate was repeated each time the diaphragm moved through 1/2 cycle. The number of fringes between any two null (zero fringe rates) points was multiplied by $\frac{\lambda}{2}$ to find the amplitude of

the vibrating diaphragm. The process was repeated for many frequencies and resulted in the amplitude vs the frequency response curve for that particular transducer.

This method was applied to audio range microphones and found to be satisfactory. It is expected that the results would be better with high frequency microphones since audio range devices do not apply themselves well to this method, because these microphones do not generally have reflective vibrating surfaces. When a reflector was added, the diaphragm mass was changed and the device no longer produced exactly the same frequency response curve. However, for purposes of determining the feasibility of the method, audio range microphones were quite satisfactory.

The curve shown in Fig 6 represents the result of the first effort to determine the frequency response of a transducer using a laser Doppler system. This curve was produced by driving the transducer over a wide frequency range at an input voltage of 1 volt peak to peak.

Conclusion

Initial investigations appeared to show that this method should be quite satisfactory for the calibration of transducers. The problem of the addition of a reflector to the transducer should be remedied by the use of higher frequency devices because these are usually crystal or capacitance type, most of which have surfaces with sufficient reflectivity. The only obstacle that might arise will be when the size and frequency of a microphone results in a surface movement of less than one wavelength of the laser light.

Future Work

Future work will primarily involve refinement of the technique and interpretation of the data. Transducers will be employed with successively higher and higher frequency ranges, which will permit the overall results of the technique to be judged more accurately.

A SENSITIVE LEVEL

G. Cline

Introduction

This project was involved with an investigation into the feasibility of using simple interference effects to create a sensitive and accurate level. The reference plane was the surface of an oil pool which was always perpendicular to the earth's gravitational field. Although various methods of approach were considered[1], the investigation was finally directed toward establishing the characteristics, both in theory and practice, of the interference phenomenon of an optical wedge which had an oil pool for a lower surface. Mineral oil was used because its index of refraction was similar to that of glass, thus providing the proper reflectance, and it was viscous enough that the vibrational surface waves were heavily damped. A glass flat was used for the upper surface of the wedges in an arrangement as shown in Fig 7.

Fizeau type fringes were formed when the apparatus was illuminated normal to the oil with an expanded and collimated laser beam. The direction of the fringes indicated the location of the apex of the wedge, and the number of fringes indicated the magnitude of the wedge angle. Absolute level was established when the upper flat was corrected until no wedge angle was present, i.e., no fringes appeared. The surface appeared uniformly illuminated when a perfect level was achieved.

Work Performed

The following calculations indicate the characteristics of the fringe pattern.

From Fig 8, if $\theta \leq 5$, $\theta = \frac{\lambda/2}{L} = \frac{\lambda}{2L}$ radians $= \frac{\lambda}{2L}\ 2.06 \times 10^5$ sec. If $\lambda = 6328$ $\overset{\circ}{A}$, then $\theta = 6.52/L$ sec. for L in cm. For the minimum detectable angle, if there was one half of a fringe (bright to dark pattern) across the flat, the

angular separation of the liquid and flat was $\theta = \frac{\lambda}{2L}$ where L was the fringe separation (in this case equal to twice the diameter of the flat), or $\theta = \frac{\lambda}{4d}$ where d = diameter of the flat in cm. Therefore, $\theta = 3.26/d$ sec. for 6328 $\overset{o}{A}$ light. The wavelength and the diameter of the flat obviously determined the ultimate sensitivity, since there were no detection problems. For example, for one half of a fringe, if d = 3.26 cm., θ = 1 sec; if d = 6.5 cm. θ = 0.5 sec. However, if a 10 per cent variation of the bright to dark pattern was detected, then θ was determined to .05 sec. using the flat of d = 6.5 cm. The limit of sensitivity is yet to be established and will probably be determined by the quality of the optical components.

A diagram of the experimental apparatus is shown in Fig 10. The laser beam, expanded to a diameter of 4 inches, was directed downward by a 45 degree beam splitter through an aperture and onto the wedge. The scanner furnished a variable aperture that scanned the periphery of the beam, and therefore allowed only a narrow shaft of light to illuminate the wedge. This shaft of light formed interference bands, shown in Fig 8, over the small area that was determined by the cross-sectional area of the aperture. The interference pattern was reflected back through the aperture, the partially reflective mirror, and was focused on a detector. As the scanner rotated across the fringes, an AC signal was generated at the detector. From this signal the magnitude and direction of the off-level were determined as illustrated in Fig 9. Point A is a fiduciary mark, the area at B is scanning parallel to the interference bands, and C is scanning across the interference bands.

Present difficulties include lack of parallelism of the beam and the apparent bending of the floors as personnel move about in the laboratory. Stable fringes are desired for the initial tests and alignment.

Future Work

Future work will consist of the development of an effective readout device, the design of which is in the early stages of planning, and the upgrading of the optical system to reduce distortion and noise level.

Reference

1 Previous report to NASA under Research Grant NsG 713 April 27, 1965

LONG PATH CELL FOR MEASUREMENT OF WEAK OPTICAL ROTATION

C. Young

Introduction

The small divergence of the laser beam was conceived to be useful in making measurements of optical rotation over large path lengths which would increase the total optical rotation available for measurement. This device would be particularly useful for measuring very small rotations. Such small rotations might be produced either by a substance exhibiting weak optical activity or by a substance showing a small Faraday effect.

In order to make these long path length measurements practical, it will be necessary to fold the optical path into a reasonable length by reflection.

Work Performed

The first experimental investigation was involved with the "first order" effects of reflection upon the apparent orientation of the plane of polarization as observed from various angles in a mirror. The experiment was performed with a laser beam reflected from a metallic mirror. The orientation of the plane of polarization was located visually by using a sheet of "Polaroid" material. The observed orientations, which appeared to correspond to the orientations of the image of the laser, were plotted on the surface of a sphere, using dashes to represent these orientations. The loci of the line segments were described by the intersection of a family of planes with the sphere. One axis of these planes was parallel to the corresponding axis of the plane of polarization before reflection, and all of the planes passed through the point on the sphere diametrically opposite the point at which the laser beam entered the sphere before reflection. The configuration is indicated in Fig 11 (a top view of the sphere) and Fig 12 (a side view of the sphere).

The first-order effect of the reflection of polarized light appeared to present to the observer a simple right-left reversal of the angle of the plane of polarization, provided that the observer used the plane fixed by the source, the mirror, and the point of observation as the "horizontal reference plane". Therefore, two reflections in series restored the original orientation.

It might appear that the simplest way of making a long path cell would be to reflect the light directly back through the solution from a single mirror and determine the right-left relation by counting the reversals. However, it is a consequence of the right-left reversal that the optical rotation presented by the beam on its first pass is cancelled out on its second pass. When the beam was reflected twice before returning through the solution, the rotation of the second pass was added to that of the first pass. This occurrence was verified experimentally.

A study of the literature concerning metallic reflection revealed that there was an effect more subtle than the "first-order" effect previously described. This effect is associated with the fact that a mirror does not equally reflect the components of the light parallel to the plane of incidence ("p" component) and perpendicular to the plane of incidence ("s" component). This unequal loss for the "p" and "s" components causes the plane of polarization of the reflected beam to be rotated from the orientation that would otherwise be expected. This situation suggests that the use of metallic mirrors should be avoided, and the total internal reflection of a prism should be used instead.

Continued study of the literature revealed that there is a very serious problem associated with the use of internal dielectric reflection. This problem is a phase shift that occurs between the "p" and "s" components of the light, so that the light after reflection is no longer plane polarized, but elleptically

polarized. This problem also occurs with metallic reflection, but is less noticeable at most angles of incidence. This phase shift will have to be compensated before the beam can be allowed to make the next pass through the solution.

There is a way that this compensation can be accomplished. Plates cut from anisotropic materials (such as quartz, calcite, or mica) have two different refractive indices, depending on the direction of vibration of light in the material. Thus one component of the light can be "slowed down" with respect to the other. This principle is used in making quarter-wave and half-wave plates. The use of such a plate is illustrated in Fig 13. Only a thin plate is actually required to produce any relative phase shift, but a thicker plate would be advisable so that it would have adequate mechanical strength. The extra thickness would merely shift the phase by multiples of 2π. The thickness relations for the plate can be given as follows:

Let

δ_1 = total phase shift between "s" and "p" components (may be $\geq 2\pi$)

δ_2 = relative phase shift of "s" and "p" components ($\leq 2\pi$)

d = thickness of plate

λ = wavelength of light in a vacuum

N_o and N_e = two refractive indices of the anisotropic plate

N = number of complete cycles of phase shift produced by extra thickness of plate required for mechanical strength

$$d = \frac{\delta_1 \lambda}{2\pi (N_o - N_e)}$$

$$d = \frac{(2\pi N + \delta_2) \lambda}{2\pi (N_o - N_e)} \qquad (1)$$

Of course, δ_2 is selected to compensate exactly for the phase shift that occurs on reflection. It is suspected (but not yet been proven) that the phase shift can be varied by rotating the compensator plate. This rotation is a degree of freedom that is needed in order that the design of the cell not have exceedingly close tolerances.

Another idea for making the required phase compensation is to use a prism made of an anisotropic material with the correction occurring in the portion of the path lying between the two faces of a given prism. The length of the path depends upon its distance from the apex of the prism, as shown in Fig 14. The adjustment can be made optically without moving the laser, by using refraction through a plane-parallel plate.

Conclusions

In order to be workable, the long path cell must be considerably more complex than that which was originally conceived. The practicality of the cell will depend largely upon the availability and price of suitable compensator plates. This problem is being investigated.

ANGULAR ALIGNMENT DEVICE

J. McElroy

Introduction

This phase of study involves the feasibility of constructing an angular alignment device using a cw gas laser and two plane front surface mirrors as shown in Fig 15.

The first mirror, M_1, was situated in a plane perpendicular to the laser beam, and the second, M_2, was at some angle ϕ with M_1. The beam was transmitted through M_1 and was incident on M_2 at this angle. The beam was then reflected between the two mirrors, forming a series of images which converged into one image as the angle between the mirrors was reduced. The operation of the device depended upon the detection of this converging action.

The fact that the images on both mirrors were available for readout added to the versatility of the device.

Work Performed

It was calculated that if L, the distance between the mirrors at the point of rotation of M_2, was held constant and the images on M_2 were numbered as shown in Fig 15, the distance, Xn, from the center of the image at zero to the center of the nth image (n=1,2,3,etc) was given by

$$Xn = 2L \frac{\sin 2n\phi + \sin 2(n-1)\,\phi + \sin 2(n-2)\,\phi \ldots + 0}{\cos\,(2n+1)\,\phi} \qquad (1)$$

Hence if L is known and Xn can be measured, ϕ can be determined from a plot of Xn vs ϕ.

The reference to the centers of the different images was necessary since each image was larger than the preceding image, because of the inherent divergence

of the laser beam. By taking this beam divergence into consideration, Equation 1 can be readily modified to relate the distance between the $\frac{1}{e^2}$ intensity points of the image at zero and the nth image.

If the angular beam divergence is α, the angle ϕ between the mirrors at which it is not possible to detect individual images is $\phi = \frac{\alpha}{2}$. This is the limit of the angle that can be determined by image position. For most commercial lasers α is on the order of 1 to 2 minutes.

A method utilizing a cube corner reflector was devised for alignment of M_1 in a plane perpendicular to the laser beam. The accuracy of the alignment of M_1 was limited by the accuracy of the angles of the reflector.

An adjustable mount for M_2 was designed and built. This mount was designed so that the center of rotation was located in the plane of the front surface of M_2. A set of mirrors has also been fabricated using plates of optical quality glass and aluminum coatings. M_1 was approximately 50 per cent reflective and M_2 was approximately 85 per cent reflective.

M_1 was initially designed with an aperture to allow transmission of the beam. This arrangement was discarded in favor of a partially reflective mirror, since at small angles the first images formed on M_1 overlapped the aperture, thus distorting succeeding images.

Conclusion

Thus far indications are that this device will apply itself to uses in which the mirrors in question are separated by a relatively large distance (5 meters).

It has been calculated that when L = 5 meters, an angle of 1 minute can be read utilizing the n = 5 image, assuming there is a beam divergence of .5 milliradians. Under these conditions the image at n = 4 is completely discernable from the image at n = 5.

Future Work

An investigation to determine the best method of detecting the image positions will be performed. There are several methods of detection under consideration at this time, and each of these will be evaluated.

The possibility of reducing or eliminating the limits imposed by the beam divergence will be investigated. It may be possible to use a lens in front of M_1 with a focal length such that the final image, n, will be approximately the same size as image zero. With this and other techniques now under consideration the ultimate sensitivity of the device should be in the range of seconds of arc.

HOLOGRAMS

G. Ballard

Introduction

The purpose of this project is to investigate techniques of obtaining images by wavefront reconstruction and to study the characteristics of the holograms from which these images are obtained.

In the wavefront reconstruction process of Gabor[1], the Fresnel diffraction pattern of an object was recorded and later used to produce an image of the original object. Such a record is called a hologram.

In recording the diffraction pattern with a single beam on film, the phase of the incident illumination is lost. With a two beam interferometric process, a transparency is placed in one beam and the second beam, acting as a carrier, is superimposed on the transparency to produce a fringe pattern, yielding a hologram which preserves the phase information.

One technique for recording a dual beam hologram is shown in Fig 16. The object was illuminated with collimated monochromatic light and a Fresnel diffraction pattern of the object was formed on the photographic plate. A portion of the incident beam also impinged on a wedge and was deviated through an angle ϕ. This "reference" beam was superimposed on the lower "information" beam, resulting in a fringe pattern superimposed on the Fresnel diffraction pattern of the object. The photographic plate recorded this pattern, producing the hologram.

An image was reconstructed from the hologram as shown in Fig 17. The hologram, placed in a collimated beam of monochromatic light, acted like a diffraction grating, separating the beam into a zero order and two first order beams. The zero order beam contained two images, similar to the original Gabor images. One of these images was a real image, located at the same distance, d,

that was the original distance between the object and the photographic plate when the hologram was recorded. Also present was a virtual image, which was out of focus with the real image and inseparable from it.

One of the first order beams produced a real image, in the same plane as the conventional real image, but displaced by the angle ϕ. The other diffracted beam produced a virtual image, as shown in Fig 17. The displaced real image was recorded by placing a photographic plate in the image plane.

Work Performed

Two problems were confronted in this project: the film to be used and the arrangement of the apparatus.

Kodak Panatomic-X film was originally selected for recording the holograms. This film is sensitive to 6328 $\overset{o}{A}$ light, and has very high resolution (136 to 225 lines/mm).

Assuming a mid-range resolution 180 lines/mm, and using the formula

$$n\lambda = d \sin \phi$$

where $n = 1$

$\lambda = 6328 \overset{o}{A}$

$d = \frac{1}{180}$ mm/line

It is found that ϕ is 6.550 degrees. This angle, ϕ, was the maximum angle that the film could resolve. This angle could probably not be realized since the interference lines of the hologram are not straight and regular but vary with each object.

It was soon found that the resolving power of the film was not the limiting factor of ϕ. The intensity of a given area of the reconstruction decreased as it was removed from the zero order beam. Thus, for larger angles of ϕ, the image was so dim that it was indistinguishable from the background light.

Kodak Contrast-Process Panachromatic film was found to give brighter images than Panatomic-X, but not enough brightness was gained to allow use of significantly larger $\emptyset$'s. Since the resolving power of the Contrast-Process film is the same range as that of Panatomic-X, the gain in brightness was evidently due to its higher contrast. Contrast-Process film has been used for recording most of the holograms.

As for the apparatus, an arrangement as shown in Fig 16 was tried first. This arrangement was relatively simple to set up, but the size of the object was limited to one-half the beam diameter, and the required wedge had to be the same size as the object. If the incident light was not accurately collimated, astigmatism was introduced by the wedge.

A pair of mirrors, arranged as in Fig 18, was preferable to a wedge for obtaining the reference beam. Here again, only half the beam was available for the object. Also, with this arrangement it was impossible to place the system on the optical bench without exceeding a $\emptyset$ that gave images that were indistinguishable from the background.

A beam splitter, positioned as in Fig 19 allowed use of the entire beam diameter for the object, although the internal reflections of the beam splitter resulted in multiple images. These multiple images were eliminated by spatial filtering, but geometry limited $\emptyset$ to a relatively large angle.

The most satisfactory arrangement found thus far is shown in Fig 20. A small prism and lens were used in the reference beam. The lens caused the beam to be brought to a focus and the pinhole minimized the aberrations that were present. The reference beam was attenuated somewhat, but this was not a severe disadvantage, since a large portion of the beam illuminated the object.

When a diffuse material was placed between the source and the object, the object was illuminated with diffuse coherent light. With holograms made in this manner each point of the object illuminated the entire photographic plate and only a small part of the hologram needed to be illuminated to reconstruct the entire image. The entire reconstruction was observed with less than 4 per cent of the hologram illuminated. This image was dim but could easily be recognized.

Both first order images were focused on a photographic plate and recorded by using diffuse illumination of the object in the arrangement shown in Fig 20. This effect was similar to the results obtained when reconstructing a Fraunhofer diffraction hologram[2]. However, in a Fraunhofer reconstruction, both images were focused in a single plane in space, whereas the images obtained in this study were in focus in different planes. Two images were observed by looking into the hologram as if it were a window.

All reconstructed images observed thus far exhibited an intensity gradient. The farther a given point of the image was from the center of the zero order beam, the less intense it became. This lack of intensity was most noticeable for reconstructions of larger objects.

There was a significant amount of background light superimposed on the image. This background had the same grainy appearance that one detects when coherent light illuminates a surface.

The real images could be focused in any plane by adjusting the collimating lens of the optical system. (As an aid in locating very dim reconstructions, this lens can be moved so as to condense the image to a small area which is more intense than the in-focus image.)

Future Work

Additional investigation into the improvement of techniques in recording both the hologram and its reconstruction should result in higher quality images.

The hologram has potential as a decision making information filter that is able to transmit patterns similar to the one that was used to make the hologram and to filter out any other patterns present. Investigation will be made into the discriminating ability of the hologram, and the manner in which variations in size, shape, and rotation of the pattern would affect this characteristic.

References

[1] D. Gabor, Proc. Roy. Soc. (London) A 197, 454, (1949)

[2] E. Leith and J. Upatnieks, J. Opt. Soc. Am. 54, 1295 (1964)

PRESSURE DETERMINATION BY RAYLEIGH SCATTERING

J. G. Dodd

Introduction

This project involves a mathematical investigation of the feasibility of using Rayleigh scattering to determine absolute pressure. Laser properties involving monochromaticity, extremely high intensity pulses, and the highly collimated nature of the emission have made possible the proposed application to high vacuum measurement. Combinations of these properties, depending upon the particular mode of operation, offer a potential breakthrough in high vacuum measurements.

The work performed thus far in this project consists of a mathematical investigation into the feasibility of using Rayleigh scattering to determine these measurements of pressure.

Work Performed

Several studies[1,2] show that when a beam of light is incident on an assembly of particles, as shown in Fig 21a, the intensity, I, of the scattered light in either watts/cm^2 or photons/cm^2/s is given by

$$I = A\, I_o\, N \frac{k^4 \alpha^2}{r^2} \sin^2 \theta \qquad (1)$$

in which $k = \frac{2\pi}{\lambda}$, α is the polarizability, A is the beam area, and N is the target atom density in number/cm^3. The intensity, therefore, is independent of ϕ.

If the system is observed in the direction of polarization, the scattering appears to be isotropic in the plane. Figure 21b shows lines of constant intensity viewed from above (the Z axis extends out of the page), and Fig 21c shows the same lines viewed from the side(the X axis extends out of the page).

If the scattered light is observed along the direction of propagation, an intensity pattern identical to Fig 21c can be seen. The amplitude of the scattered light reflects the angular dependence of the polarization vector. The quality P in Fig 21c must be rotated by 90-Θ from P_Z, the incident beam polarization, because polarization is "conserved" and waves are always polarized perpendicularly to their direction of propagation. Therefore, E(P) must be the component of P_Z in the direction perpendicular to r, or E (P_Z) sin Θ. Since intensity is proportional to the square of amplitude,

$$I \propto E^2 (P) = E^2 (P_Z) \sin^2 \Theta \qquad (2)$$

This equation is the origin of the $\sin^2 \Theta$ term in Equation 1. The pattern for Rayleigh incoherent scattering is a holeless doughnut, and it is symmetric to the polarization direction but independent of the polar angle ϕ.

In order to obtain a fixed solid angle of acceptance by the detector, more of the beam can be observed when ϕ is close to zero or π. The assumption of incoherent scattering, which is safe for ordinary beams, must be re-examined when it is used in connection with lasers[3] because the behavior is different. The variation in scattering as a function of ϕ (which should show a minimum at $\phi = 60^o$) only amounts to approximately 20 per cent of the total intensity. There is another term, of unknown origin, which favors small and large ϕ's and is as important as the coherent term. Therefore, it is necessary to write a three-term expression for the scattered intensity[3]:

$$I_H = \left[(I_{inc} + I_{coh}) \cos^2 x + I^H_{sym} \right] \times 0.48 \qquad (3)$$

where I^H_{sym} is an empirical term.

The ordinary incoherent scattering term is unaffected by the other terms (which are intrinsically positive) and therefore represents the minimum scattering intensity. Although Equations 2 and 3 may be helpful, they will be ignored for the present time.

The next phase of this investigation involved the calculation of anticipated photon flus. If a beam of monochromatic light of wavelength λ is directed into a gas of polarizability α and molecular density N/cm^3, then the light flux equals AI_o, which equals P photons/s.

A light pipe, such as the one shown in Fig 22a, will gather all of the light scattered from the beam and deliver it to the phototube with the efficiency, ϵ, with the only loss of light being out of the ends. The trumpet-shaped light pipe is solid lucite and is completely silvered on the outside. The hole in the apparatus must be all the way through to admit the beam and should have a diameter of one cm.

This light pipe has the following advantages: (1) All of the entering light is effectively trapped; (2) scattered light from the outside cannot enter; (3) the light pipe can be made on a lathe; and (4) it is compact and easy to pump down. It is not believed that the shape of the light pipe is too critical. Since total internal reflection is more efficient than specular reflection, one should try to obtain it as often as possible.

The flux delivered to the photomultiplier will be

$$F = \epsilon P \int_V \int_A \frac{k^4 \alpha^2 \sin^2 \theta}{r^2} \, da\,dv \qquad (4)$$

in which A is the internal area of the hole; and $dv = a\,dx$, where a is the beam cross-section.

The integration can be set up from Fig 22b; then the contribution from dv into da will be

$$d^2I = \epsilon \frac{NI_o k^4 \alpha^2}{r^2} \cos^2 \theta \cos \phi \, \rho\, d\theta\, dZ\, a\,dx.$$

$$r^2 = (x + z)^2 + \rho^2 \qquad \cos \phi = \frac{\rho}{\sqrt{(x+z)^2 + \rho^2}} \qquad (5)$$

Thus

$$F = ca\, NI_o\, k^4\, \alpha^2\, \rho^2 \int_{-\frac{L}{2}}^{\frac{L}{2}} \int_{-\frac{L}{2}}^{\frac{L}{2}} \int_0^{2\pi} \frac{\cos^2 \theta \, d\theta \, dxdz}{(x+z)^2 + \rho^2} \tag{6}$$

Carrying out the integration,

$$F = 2\pi\, a\, \rho\, \epsilon\, NI_o\, k^4\, \alpha^2 \left[\sqrt{\rho^2 + L^2} - \rho \right] \tag{7}$$

$I_o a$ is the beam flux in photons/s. The flux, F, which is scattered into the detector, is also in photons/s.

It is known that even the best photon detector has some quantum efficiency, q, and noise level, n photons/s. The detected flux is

$$F_d = qF \tag{8}$$

If the least count of the system to be given by the flux, F, will generate a 2:1 (signal + noise)/noise ratio, then

$$\frac{F_d + n}{n} = \frac{qF + n}{n} = 2 \tag{9}$$

F min $= \frac{n}{q}$; to determine the lowest detectable pressure:

$$(N)_{min} = \frac{n}{2\pi a \rho \epsilon\, NI_o\, k^4\, \alpha^2 \left[\sqrt{L^2 + \rho^2} - \rho\right]} \tag{10}$$

Example: If a one-watt cw laser is used, then $(I_o a)\, \frac{hc}{\lambda} = 1$; $I_o a = \frac{\lambda}{hc}$.
Since $\lambda = 6328$ Å for a He-Ne laser,

$$I_o a = 2.86 \times 10^{18} \text{ photons/s}$$

$$k^4 = \frac{(2\pi)^4}{\lambda^4} = 9.3 \times 10^{19} \tag{11}$$

It will be assumed that $\epsilon = 0.5$; q and n are given[4] as $\simeq .05$ and $\simeq 15$ counts/s respectively for the cooled 9558 photomultiplier.

In order to calculate the polarizability, the following relation[4a] can be used:

$$n^2 - 1 = 4\pi N \alpha \tag{12}$$

For nitrogen, as well as most gases at N.T.P., $n \gtrsim 1$.

Thus $\quad n^2 - 1 = (n-1)(n+1) \simeq 2(n-1)$

Hence $\quad n - 1 = 2\pi N \alpha$

$$\alpha = \frac{n-1}{2\pi N} \tag{13}$$

For nitrogen[5] at 760 mm, 0° k, $n-1 = 2.919 \times 10^{-4}$ and $N = 2.78 \times 10^{19}$ cm^3.

Thus $\quad \alpha = 1.67 \times 10^{-24}$ cm^3 (14)

Assume that L = 30 cm and ρ = 1/2 cm. Then

$$\sqrt{\rho^2 + L^2} - \rho \simeq L = 30.$$

Inserting this into Equation 10,

$$(N)_{min} = 8.6 \times 10^9 \text{ molecules/cm}^3 = 2.3 \times 10^{-7} \text{ mm}$$

This result is deceiving for two reasons: in the first place, the entire system is absolutely optimum, and secondly, this is a le t count figure. The pressure could be detected but not measured. The count rate would be approximately 15 counts/s above a background of 15 counts/s.

High-power pulsed lasers offer another possibility for improved performance. If the laser frequency is doubled, resulting in an efficiency of 0.2, then the $\frac{1}{\lambda^4}$ power Rayleigh law can be employed to produce a net gain. Three factors are changed by this procedure: (1) the photon flux is down to 0.1, i.e., the photon number is halved with the conversion efficiency of 0.2, (2) the Rayleigh cross-section is up by 16, and (3) the quantum efficiency of the photomultiplier may be raised as high as 0.2. The noise may be lower for blue-sensitive cells also, but there is no information available on this. In any case, the net result is the changing of $(N)_{min}$ by the factor.

$$N = (N)_{min} \frac{\lambda^4 q_o I_o}{\lambda_o^4 q(1/2\ I)} \tag{15}$$

in which the subscripted quantities are the original ones for 6328 Å light, and the new quantities are not subscripted.

Then $\frac{\lambda^4}{\lambda_o^4} = \frac{1}{16}$, $\frac{q_o}{q} = \frac{1}{4}$, $\frac{I_o}{(1/2\ I)} = 10$ to yield

$$N = (N)_{min}\ \frac{10}{64} = 3.6 \times 10^{-8} \text{ mm Hg} \qquad (16)$$

The resulting gain is larger than one order of magnitude.

This problem is essentially a statistical one. The least count of the system, N, is determined by the reliability with which Equation 9 can be evaluated. The noise count rate, n, and the signal count rate, F, are statistical quantities. If these quantities follow the Poisson distribution, the probable deviation in a mean count of n_o will be $\sqrt{n_o}$ [6]. In other words, if the noise rate is 15 counts/s, the rms deviation that is expected in a one-second count is $\pm$ 4 counts/s. One must go to higher integrating periods in order to obtain better statistics. The following equation is required if a one per cent deviation in the count rate of a 2:1 s +n/n ratio of 30 counts/s and a deviation of one per cent of 30 = 0.3 counts or $\pm$ 3 counts out of 300 are desired.

$$\frac{\sqrt{n}}{n} = .01$$

$$n = 10^{-4}\ n^2$$

$$n = 10^4 \qquad (17)$$

At 30 counts/s, a data-taking time of $\sim$350 s (about six minutes) is required.

The immediate question is whether or not an improvement can be obtained by using a Q-spoiled laser with coincidence circuitry. This possibility could be investigated with the use of a one Joule, Q-spoiled laser pulse of 3×10^{-8} s. width. Noise may be neglected because, at a noise level pulse rate of 15/s, the probability of finding even one noise pulse in such a small interval is extremely small.

The flux that the detector observes will be that which is scattered by one watt-second (1 joule) of irradiation by the one watt laser discussed previously.

As was pointed out in Equation 16, this flux for a pressure of 3.6×10^{-8} mm Hg (including the gain by doubling) is only 15 counts at the read-out counter. The requirement of one per cent deviation in the s + n count number implies approximately 1.2 per cent standard deviation in each equal s and n count rate. This deviation is exactly the same that might be expected in $\frac{500}{15} = 33.3$ pulses of the Q-spoiled laser. One pulse, yielding $\sim$15 counts of scattered radiation at 3.6×10^{-8} mm, would have an uncertainty of $\pm$ 4 counts. The above uncertainty is for a noise-free 15 count signal.

Therefore, there is no theoretical advantage in Q-spoiled lasers with coincidence circuitry over cw techniques, although there may be a practical advantage. Uncooled photomultipliers have high dark currents, in which typical figures are equivalent to several thousand counts/sec; and cw techniques obviously require cooling. Pulse lasers, however, can use gating pulses of $\sim$1 μ sec. to turn on the photomultiplier; and in this period of time the probability of admitting a single noise pulse, even for an uncooled photomultiplier, is less than one. In addition, the photomultiplier will not resolve the signal pulse, which will appear as a large pulse compared with noise pulses. Therefore, pulse height discrimination can be used.

The differential cross-section for a scattering process such as Rayleigh scattering is defined by the equation

$$\frac{d\sigma}{d\omega} = \frac{1}{N} \frac{I r^2}{I_o} \quad . \quad \text{cm}^2/\text{unit solid angle} \qquad (18)$$

From Equation 1, the right side can be written in terms of the polarizability, wave number, and angle θ as:

$$\frac{d\sigma}{d\omega} = k^4 \alpha^2 \sin^2 \theta \qquad (19)$$

The total cross-section for Rayleigh scattering through any angle is

$$\sigma_t = \int_{4\pi} \frac{d\sigma}{d\omega}\, d\omega = k^4 \alpha^2 \int_{4\pi} \sin^2\theta \cdot \sin\theta\, d\theta$$

$$= \frac{8\pi}{3} k^4 \alpha^2 \qquad (20)$$

According to the terms in either Equation 19 or 20, the intensity per unit beam volume which is scattered into a unit solid angle ($I\omega$) or into a 4π solid angle (I) can be written:

$$I\omega = \left(\frac{d\sigma}{d\omega}\right) \cdot NI_o \qquad (21a)$$

$$I = \sigma_t\, NI_o \qquad (21b)$$

In Equations 21a and 21b the particle picture of radiation is considered, and I_o is imagined as being measured in photons/s/cm^2. Therefore, σ_t or $\frac{d\sigma}{d\omega}$ represent the apparent "size" of the molecule as seen by the incoming photon. In Equation 19 or 20, these parameters are seen as apparently smooth functions of the wavelength; although this condition is true only when the parameters are far from characteristic excitation energies. In general it must be written:

$$\sigma_t = \frac{8\pi}{3} r_o^2 \left[Z_1 - \sum_k \frac{(h\nu_k)^2 f_k}{(h\nu_k)^2 - (h\nu_o)^2} \right]^2$$

$$= = \frac{8\pi}{3} r_o^2 \left[Z_1 - \sum_k \frac{f_k \big/ \lambda^2_k}{\frac{1}{\lambda^2_k} - \frac{1}{\lambda^2_o}} \right]^2 \qquad (22)$$

in which the oscillator strengths, f_k, are the probabilities that if an electron in the molecule undergoes a transition from an initial state, it will go to the kth state. Obviously then

$$\sum_k f_k = 1 \qquad (23a)$$

since it must go to some state. If the molecule contains Z_1 electrons, then

$$\sum f_k = Z_1 \qquad (23b)$$

The parameter $r_o = \frac{e^2}{mc^2}$ is the classical radius of the electron. In Equation 22, the λ_k are characteristic absorption lines or bands, and the irradiating wavelength is λ_o. Three interesting cases are shown below. The first, $\lambda_k >> \lambda_o$, yields

$$\sigma_t \cong \frac{8\pi}{3} r_o^2 \left[Z_1 + \frac{\Sigma f_k}{\lambda^2_k} \lambda_o^2 \right]^2 \qquad (24)$$

Physically, such a situation can arise only if low energy transitions predominate. The extreme case is the free electron, in which all λ_k are zero. Thus

$$(\sigma_t)\ \text{electron} = \frac{8\pi}{3} r_o^2 \ Z_1^2 \qquad (25)$$

This equation is the Thompson scattering cross-section for free electrons, and it is independent of incident wavelength.

The second case arises if $\lambda_k << \lambda_o$. In this case the numerator and denominator of the fraction under summation by λ_k are multiplied and expanded by the binomial series to obtain:

$$\sigma_t \cong \frac{8\pi}{3} r_o^2 \left[Z_1 - \Sigma f_k \left(1 + \frac{\lambda^2_k}{\lambda_o^2}\right) \right]^2 \qquad (26a)$$

Applying Equation 23b,

$$\sigma_t \cong \frac{8\pi}{3} r_o^2 \frac{(\Sigma f_k \lambda^2_k)^2}{\lambda_o^4} \qquad (26b)$$

which is Rayleigh scattering.

The third case offers the most interesting possibility from the point of view of gas detection. If one of the λ_k lies close to λ_o, the λ_k term will dominate the sum, and (calling this particular transition the kth)

$$\sigma_t = \frac{8\pi}{3} r_o^2 \left[Z_1 - \frac{f_k \Big/ \lambda^2_k}{1/\lambda^2_k - 1/\lambda^2_o} \right]^2 \qquad (27)$$

which is a function having the shape shown in Fig 23.

The cross-section near one of the λ_k is therefore large and theoretically infinite. This condition might be a useful gas analysis tool at low gas densities if laser wavelengths that are sufficiently close to a λ_k can be chosen. In order to gain some idea of how close such a wavelength interval $\lambda_k - \lambda_o$ might have to be, one would have to know the λ_k spectrum and the associated f_k. For example, one might get close enough to a particular λ_k that that term, in the sum of Equation 22, would be ten times its normal Rayleigh value, and it still might be small compared to other terms that dominate the scattering because of large associated f_k. Nevertheless, any transition active enough to be optically important is probably strong enough to be useful. In practice, of course, σ_t does not go to infinity at λ_k since line widths are appreciable, and the above analysis is correct only for infinitely narrow lines.

In the above investigation, the basic Rayleigh scattering equations (Equations 1, 19, 20, and 21) have been listed and one example has been given of a detailed sensitivity calculation that assumes a reasonable light collection system. Whatever geometry is chosen, the calculation of collected light flux must proceed along the lines laid out in Equations 4 through 12. Similarly, the sensitivity calculations carried out in Equations 13 through 17 are basically the same for any system of this type; only the numbers will change.

The inevitability of statistical variation of recorded counts, even neglecting system noise, should be emphasized. Signals are always made of quanta and they appear continuous only at high levels. At low levels, these individual counts are as random as those from a decaying radioisotope, and therefore they require the same statistical requirements. The standard deviation expected in n counts is $\sqrt{n}$, and there is no way to improve the accuracy of such a system except by increasing n. This restriction arises even in a perfect noise-free detection system.

The Rayleigh study by Watson and Clark[7] finds no evidence of coherent scattering effects, and the classical Rayleigh scattering pattern is fully verified. It is suggested that this article be read carefully and compared with the enclosed report or with its open literature version.[8]

References

1 Stone, Radiation and Optics, Chap 14, Sec. 2, pp 340-44 (McGraw-Hill)

2 George and Goldstein, Final Report Contract AF19(604)-7473 (AFCRL-63-549; AD 427730), p. 12.

3 Ibid, Section 3.2, pp 16-21

4 Rodman and Smith, Applied Optics 2, p. 181 (1963)

4a Ref. 1, p. 377

5 American Institute of Physics Handbook, pp. 6-95.

6 Handbook of Physics, Candon and Odishaw, pp. 1-155.

7 Watson and Clark, Phys. Rev. L. 14, p. 1057 (1965).

8 Ibid, 137, p. 369 (1965)

TEMPORARILY SUSPENDED PROJECTS

A Fast and Accurate Means of Adjusting Gas Flow Rate

This project, as was described in a previous report, in which a gas flow rate was measured by means of the Doppler frequency shift of light reflecting from the surface of a moving gas bubble, has been temporarily suspended. This suspension was done in order to allow full time concentration on the hologram project, and it will be reinstated as quickly as possible.

A Cell for Measuring the Index of Refraction of Liquids

The main body of the proposed project of investigating and developing a cell capable of measuring small changes in the index of refraction of liquids was described in a previous report. Since then the project has been temporarily suspended in order to give more emphasis to the hologram project.

Although a few minor problems have been encountered, they are not difficult enough to cause cancellation of the project, and additional work on it will be continued as soon as possible.

CANCELLED PROJECTS

MOMENTUM DETECTOR

P. C. McLeod

Introduction

When a laser beam is employed in a typical interferometer, small movements of the reflecting mirrors can be observed as interference fringes, which occur rapidly if the velocity of the reflecting surface is high. For example, if the reflecting surface is moving toward the laser beam at a rate of one centimeter per second, the fringe rate would be approximately 30,000 fringes per second. (This technique, of course, is the Doppler method of measuring velocities.) If the movement of the reflector was due to a collision between the reflector and a small particle, the velocity of the combined pair could be monitered as a Doppler frequency shift, resulting in an effective measure of the momentum of the particle that caused the reflecting surface to be disturbed, provided the characteristics of the reflector are known.

Work Performed

The experimental apparatus was set up as shown in Fig 24. There was one limitation at the time testing began, that being the frequency response of the photodetector and its supporting electronics. Since it is desirable to keep the electronics in the RF range, the reflector velocity should never exceed 100 meters/second, which is equivalent to approximately 300 megacycles/second frequency shift. During testing, however, a second and extremely severe limitation appeared. This limitation involved the inability to maintain optical alignment during the time that the reflecting surface, in this case a diaphragm, was being deflected. The seriousness of this problem may be seen by the fact that the test velocities were on the order of 100 cm/second or roughly

one per cent of the allowable maximum velocity. The particles used were spherical with a mass range of 2 to 122 milligrams resulting in a range momenta from 9.17 to 14.00 dyne-centimeters. The only time during the tests that Doppler effects could be observed was when the particle hit the diaphragm at the center of the laser beam so that the beam alignment was not lost. Under these conditions sensitive measurements of momentum can be accomplished but the device depends upon an extremely small sampling area. One of the methods employed to remedy this problem was diffused beam techniques; however, under all conditions, intensity changes due to loss of alignment were serious.

Conclusions

Methods employed in existing momentum detectors were reviewed to see if laser techniques could be incorporated. It is doubtful that the use of a laser would increase the sensitivity or range of measurements enough to warrant the additional complication necessary to incorporate a laser into exisitng devices. Therefore it was decided that this investigation should be terminated, even though a great deal of experience was gained in observing moving bodies by interferometric methods. Other uses of this technique will be considered since it allows the measurement of the velocity, displacement and period of a vibrating body at considerable distances and requires only the reflection of a laser beam to achieve these measurements.

VARIABLE OPTICAL DELAY LINE

J. McElroy

Introduction

A variable optical delay line was proposed to be built utilizing multiple reflections between a pair of plane, front surface mirrors situated in a parallel, face to face configuration as shown in Fig 25.

A ray of light incident on mirror 1 at an angle ϕ will be reflected at the same angle. Since the mirrors are parallel, the ray will be incident on mirror 2 at the same angle.

The distance traveled by the ray during one round trip (two reflections) is $\frac{2d}{\cos \phi}$. During this time the ray will be displaced horizontally from A to B, the distance being 2d tan ϕ. The number of round trips that the beam makes between A and C is given by $\frac{L}{2d \tan \phi}$, where L is the distance from A to C. The total distance traveled by the ray is the number of round trips times the distance traveled per round trip, or $S = \frac{L}{2d \tan \phi} \frac{2d}{\cos \phi} = \frac{L}{\sin \phi}$. The time required to travel this distance is $t = \frac{L}{C \sin \phi}$ where C is the velocity of light.

Work Performed

A pair of adjustable mirror mounts was fabricated and attempts were made to create a predictable delay. It was found that, in order for all the reflections to remain in a plane perpendicular to the reflecting surfaces, the mirrors had to be of high quality and adjusted critically.

The possibility of using spherical mirrors was investigated, but it was found that Kurnitz[1] had used a similar method involving spherical mirrors with good results. With this information the project became a reduction to practice and the effort was terminated.

Reference

[1] Kurnitz, Abella, and Hartamann, Phys. Rev. Letters 13; 567, (1964)

INVESTIGATION OF LASER AND DIAPHRAGM AS PRESSURE TRANSDUCER

C. Young

Introduction

The properties of coherence of a laser and the ease of developing interference fringes as a function of displacement appeared to be a convenient way of gathering information from a pressure transducer when the displacement of a surface was a function of the pressure.

The form of transducer chosen for investigation was a circular membrane bounded at the circumference. Methods of excitation to be investigated included that of electrostatic force and a sound coupled driving system using a loud speaker driver unit. Sound coupling requires that the environment of the transducer and the speaker be able to propagate sound intensities.

Work Performed

A study of diaphragm mathematics was undertaken in order to provide information for a preliminary design. Since no particular advantages in diaphragm shape or size could be determined from this investigation, a circular diaphragm was chosen in preference to a rectangular form, since the driving source available was more suitable to a circular shape.

The diaphragm mount provided a means of varying and measuring diaphragm size and tension. Diaphragms used ranged from one and three quarters to four inches in diameter. The membrane was made from mylar, manufactured by the Hastings Company, which was 0.001 inches thick and aluminized on both sides. Varying thicknesses of mylar are available.

The remainder of the assembly consisted of a 16 ohm 30 watt speaker driver, which was employed as one of the driving units; standard optical supports; signal generators and matching amplifiers. The functional block

diagram of the experimental apparatus is shown in Fig 26. Figure 27 shows the data obtained from the primary mode of a circular diaphragm.

The mass of the mylar was measured and found to be 9.24 mg/cm^2, and the first diaphragm that was tested was 3-7/8 inches in diameter. Various points on the diaphragm were explored and the data was photographed. The resonant frequency was 460 cycles/sec. and 90 fringes were produced at resonance.

A smaller diaphragm of 2-1/4 inches in diameter was examined in the same manner as the above and was found to have a resonant frequency of 760 cycles/sec. and to produce 30 fringes at resonance.

It is apparent that the larger the membrane diameter, the greater the number of bits of information (90 vs 30 from the above examples) that are available for the measurement of the displacement. However, it does appear that many more bits of information would be required to measure pressure several orders of magnitude below atmospheric. In order to provide the necessary information a membrane or diaphragm would have to be larger than is practical for a useful transducer.

The resonance of the diaphragm was easily determined since a maximum number of interference patterns as a function of frequency were observed when the laser beam was modulated by the displacement of the diaphragm. Higher modes were observed when the diaphragm was vibrating at frequencies other than the fundamental. In some cases higher order vibrations appeared when the diaphragm was either over-driven or not oriented normal to the driver. It was found that when the speaker was aligned off axis, higher modes of vibration appeared on the diaphragm surface. When normal alignment to the surface of the diaphragm was accomplished, a wide range of excitation distances did not appear to excite extraneous modes and the fundamental diaphragm mode was maintained.

Conclusion

A number of problems was discovered in the course of the project. Over-driving of the diaphragm appeared to cause multiple modes, distortion in the output signal, and beats within the interference pattern. These movements could possibly be determined as warping of the membrane and movements other than simple concentric Bessels modes. The actual properties of the diaphragm when over-driven have not been determined, but it is believed that higher modes of vibration become dominant enough to cause data distortion. The distorted information was considered unreliable although more information bits were available. Each vibration was not a replica of the previous vibration and therefore would not be suitable for display or reliable data.

Several attempts to use electrostatic coupling on the mylar membrane resulted in what appeared to be the attraction of the mylar onto the voltage source. Approximately 1500 volts were used both as time varying and DC. When safe distances between the mylar and the electrostatic electrode were used, the forces were too small to get sufficient displacement to allow the measurement of pressure loading by the air. According to calculations, the contribution of gas densities add little to the damping characteristics of the membrane, providing that high modulating voltages at the resonant frequency are used. Basically then, little change in interference fringe rate could be expected of a system of this kind when used as a pressure transducer.

From the above information and the knowledge of the mathematical parameters, it is believed that the mechanics and techniques are unique and reliable within a limited range of accuracy. It is also believed, however, that with a diameter of approximately 4 inches at standard air pressure, 90 bits of information is

not enough to describe pressure down to the mm range in any detail. The damping effect of air pressure is not a large enough factor to control the vibration amplitude and frequency. Because of this information and the problems listed above, it was decided to terminate the project.

MEASUREMENT OF THE INDEX OF REFRACTION OF GASES

C. W. Young

Introduction

Some of the earliest and most accurate methods of measuring the index of refraction of gases utilized interferometric techniques. Since the continuous gas laser is readily applicable to the various types of interferometry, it was proposed that it might be possible to increase the accuracy of some of the present measurements by fabricating an accurate, precise interferometer with a laser as the light source.

Work Performed

During the investigation it was learned that many times it was not the interferometer, but the control of temperature and pressure to precise values that limited the accuracy of the measurement. It has been calculated that it would be necessary to control the temperature to within 0.001 degrees centigrade to improve the accuracy of present values. A study of many different types of interferometers and experimental work with several different configurations were performed in order to determine if there might be a particular type of interferometer that would apply itself to the measurement of index of refraction of gases in which the environment of the gas sample cell could be closely controlled. A satisfactory solution has not been found and since the problem has become an investigation of environmental control methods, the project has been terminated.

A large amount of useful information relating to interferometers and interferometry technique was gained while performing this work.

AXICON LASER ALIGNMENT SYSTEM

R. L. Bond

Introduction

It has been suggested that a long-range alignment device could be devised utilizing a laser as a light source and an axicon lens[1] to provide a well-collimated line of light, which would monitor the gradual movement of a large mass over a long period of time. The projection distance desired was at least 1000 yards. A system to accomplish this was shown to be impractical because of the size of the axicon, power requirements for the continuous laser, and the stability of detection over periods of several weeks. Emphasis was shifted in an effort to devise a "laboratory size" system.

Work Performed

An axicon lens was designed that would give a maximum projection distance of ten feet using a beam of parallel light three inches in diameter. It was calculated that a lens three inches in diameter, made of a material with a refractive index of 1.49 would require a cone angle of 177^{o} 04'. This lens was made and its calculated value of beam length agreed well with the experimental value. However, the quality of the lens was not good because a great deal of light was scattered because of surface imperfections and poor quality optical material.

Conclusion

The maximum projection distance of the axicon beam is directly related to the cone angle of the axicon and the wave front (plane or spherical) entering the axicon. A large cone angle is required for a projection distance of only ten feet. Increasing the diameter of the lens and impinging beam would increase the projection distance, but a well designed gas laser is apparently superior to

the axicon-laser system for alignment purposes over short distances. Thus it is seen that an alignment device of the axicon type would be of little value for the applications considered in this work.

Reference

[1] J. H. McLeod, "The Axicon: A New Type of Optical Element", J. Opt. Soc. of Am. 44, 592 (1954)

Figure 1

MEMBRANE SHAPES

(Theoretical and Actual
Vibrations Well Established)

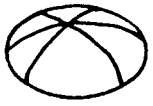

m = 0
n = 1

m = 0
n = 2

m = 0
n = 3

m = 1
n = 1

EQUATIONS

$$U(r\theta t) = \sum_{\substack{m=0 \\ n=0}}^{\infty} A_{mn} \cos m\theta \, Jm(knr) \cos kn\gamma t$$

$$\gamma = \sqrt{T/\rho}$$

T = tension

ρ = density/cm^2

$$U(rt) = \sum_{\substack{m=0 \\ n=n}}^{\infty} A_n \, Jo\,(knr) \cos kn\gamma t$$

$$\frac{Wn}{2\pi} = \frac{kn\gamma}{2\pi}$$ (Characteristic frequency relationship)

kn from Bessels Functions

TYPICAL RECTANGULAR SURFACES

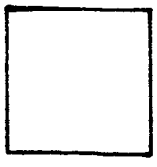

$\omega = \alpha\sqrt{2}$

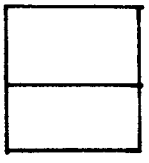

$\omega = \alpha\sqrt{5}$

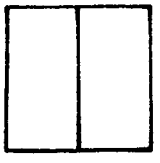

$\omega = \alpha\sqrt{5}$.

$$U(xyt) = (A \sin_{nn} \omega t + \cos_{nm} \omega t) \times \left(\sin \frac{\pi x}{a}\right)\left(\sin \frac{\pi y}{a}\right)$$

$$\omega_{mn} = \frac{\gamma \pi}{a} \sqrt{m^2 + n^2}$$

$$\alpha = \frac{\gamma \pi}{a}$$

Figure 2

BASIC POINT BY POINT SYSTEM

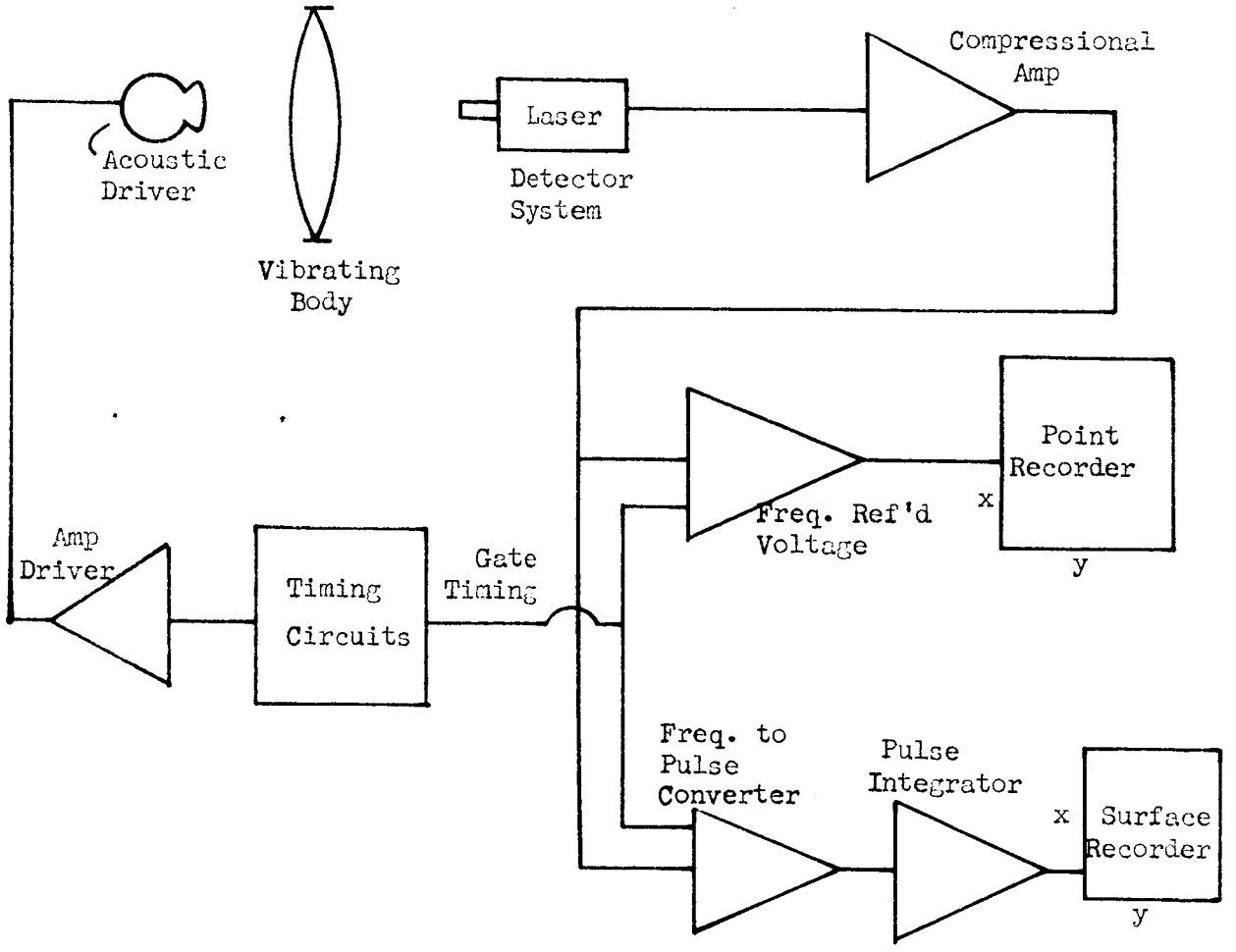

Point Recorder Data

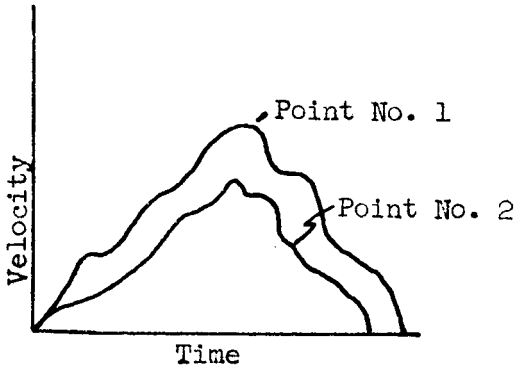

Surface Recorder Data

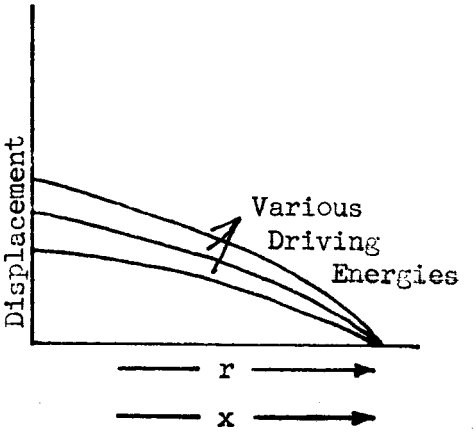

Figure 3

DIAGRAM OF A SYNCHRONOUS SYSTEM USING A GAS LASER

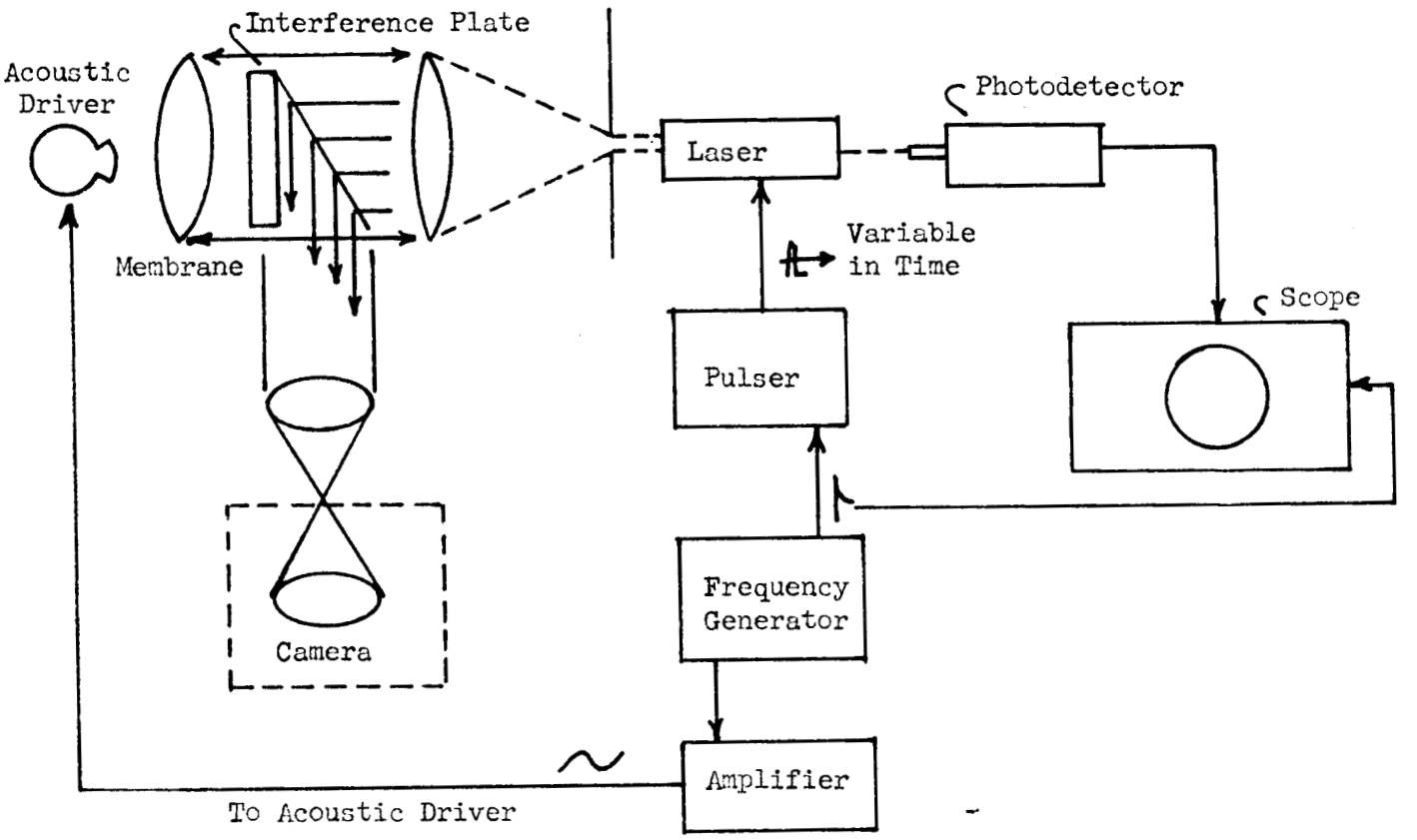

Figure 4

TIMING SYNCHROGRAM

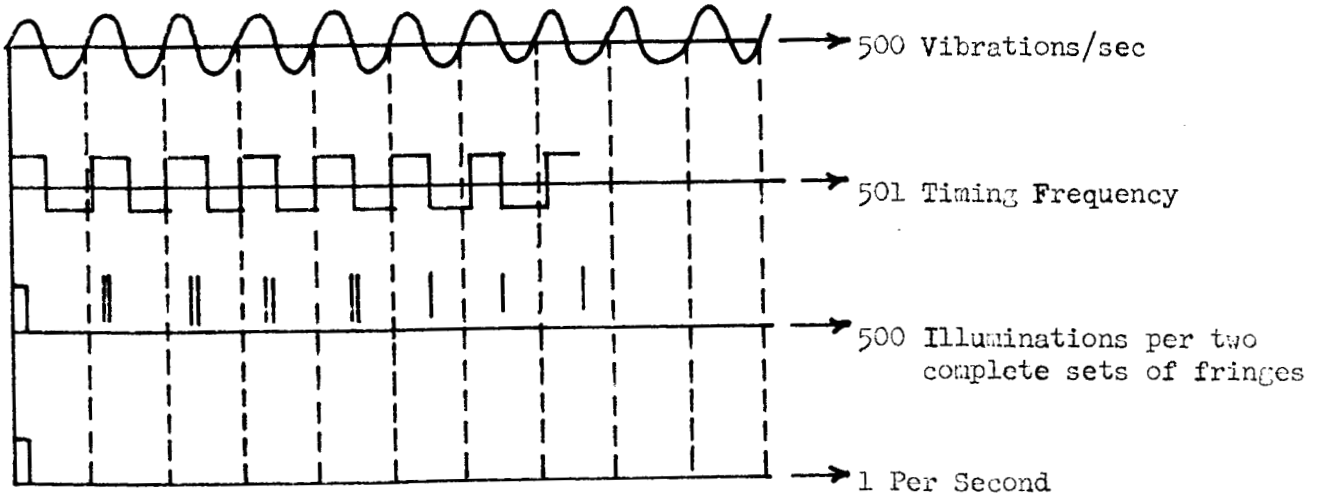

Figure 5

EXPERIMENTAL EQUIPMENT SET-UP OF LASER FEEDBACK SYSTEM

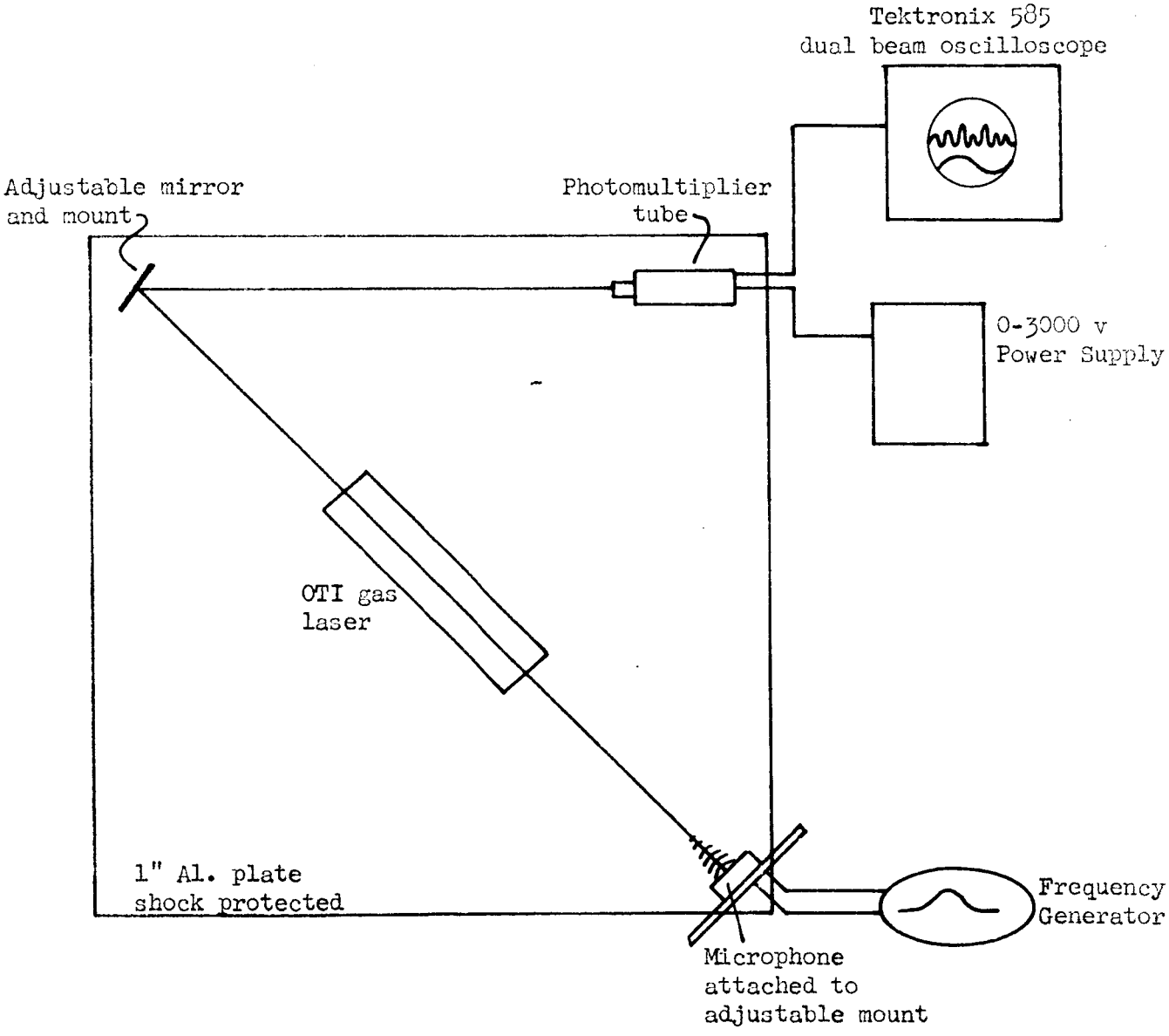

Figure 6

AMPLITUDE OF VIBRATION (EXCURSION) VS FREQUENCY

Input = 1.0 volt

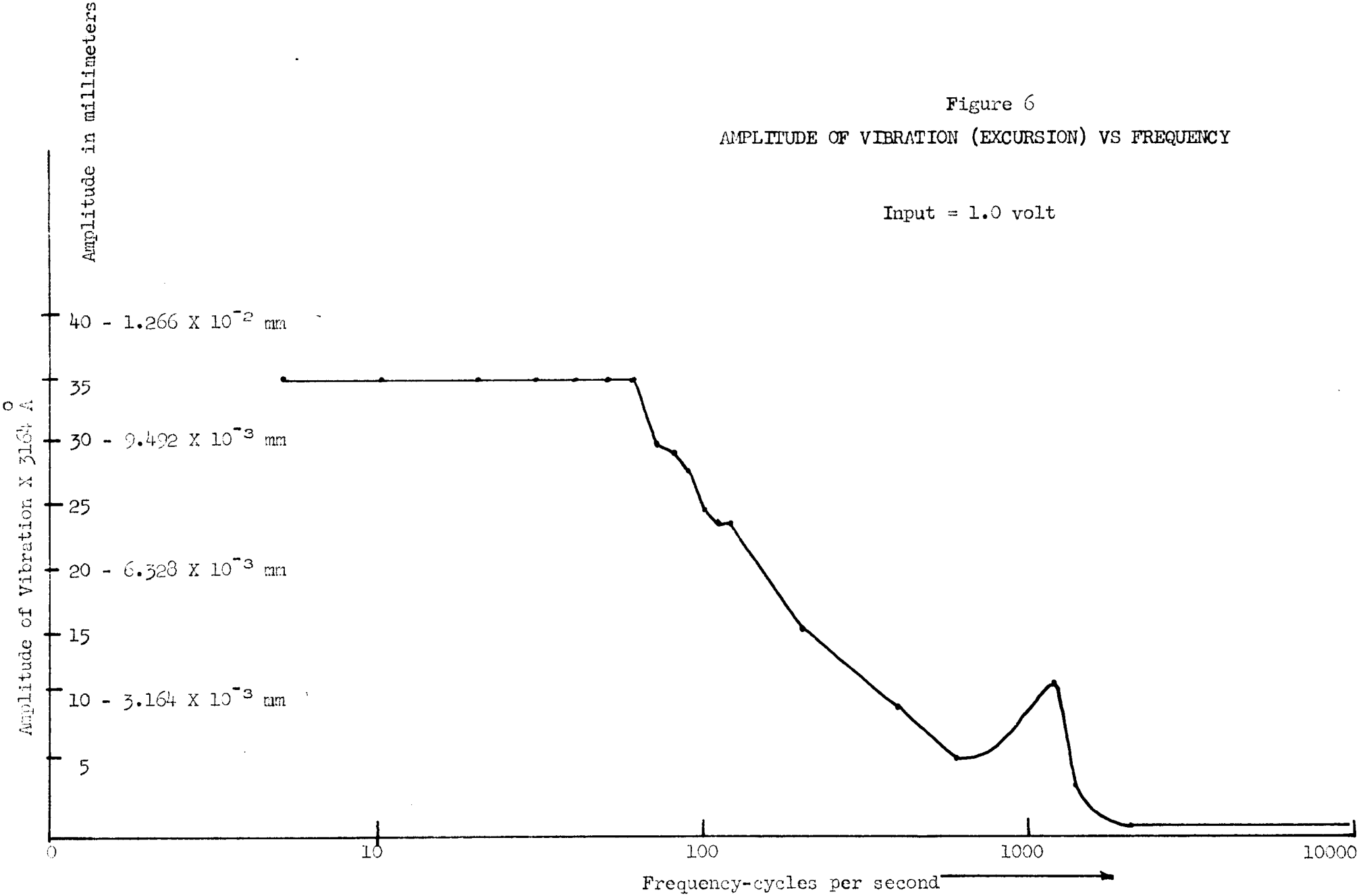

Figure 7

CONTAINER WITH GLASS FLAT

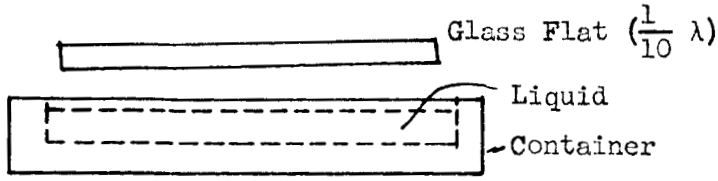

Figure 8

CHARACTERISTICS OF THE FRINGE PATTERN

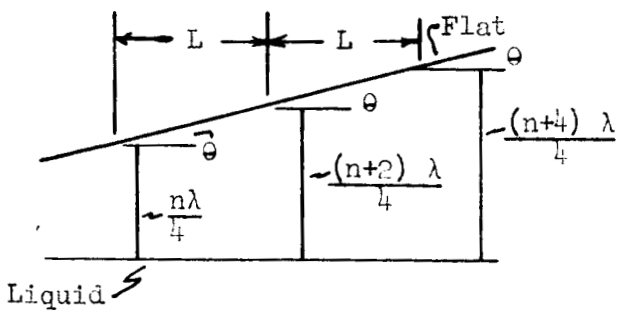

n = 1,3,5,...
λ = wavelength of light
L = distance between fringes (cm.)

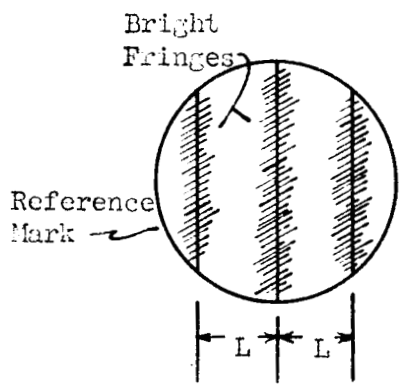

Pattern on circular flat as seen from above

Figure 9

SCOPE PRESENTATION OF AC SIGNAL

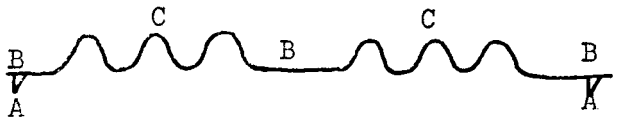

Figure 10

THE EXPERIMENTAL APPARATUS FOR LEVEL DETECTION

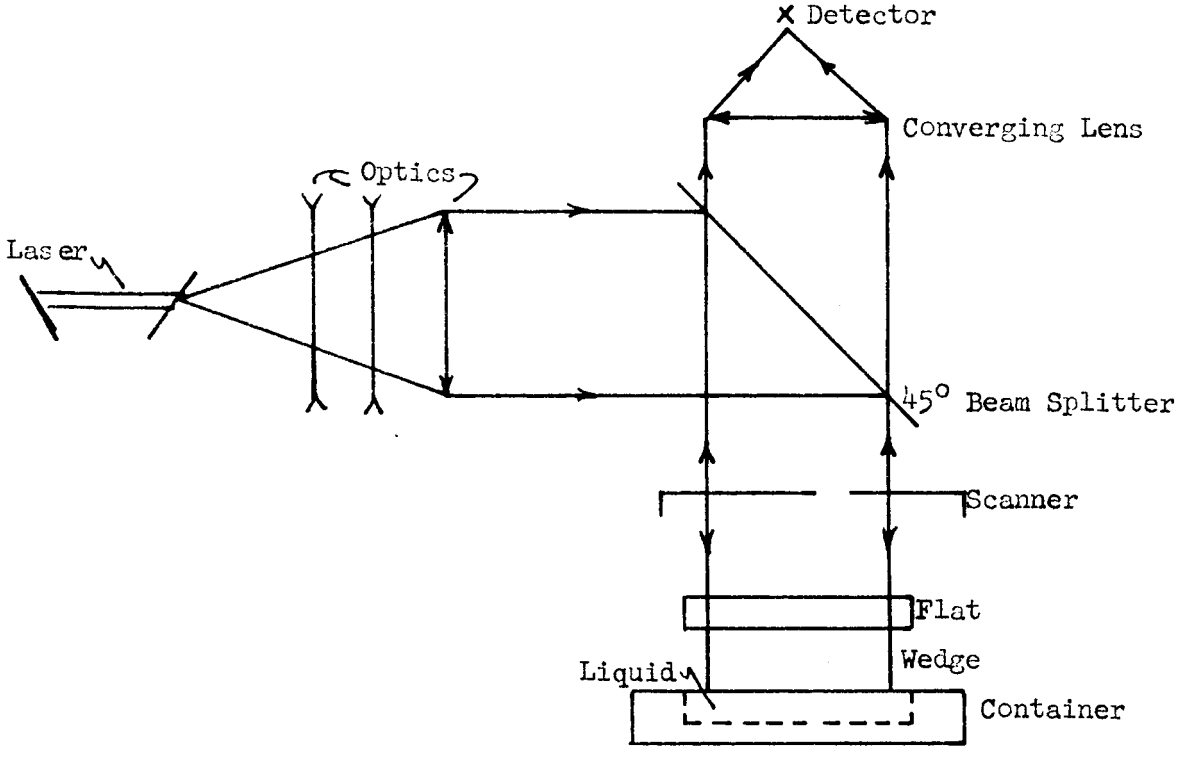

Figure 11

Top view of the sphere on which is plotted the apparent orientations of the plane of polarization of the laser beam reflected from a mirror at the center of the sphere (First order effect only)

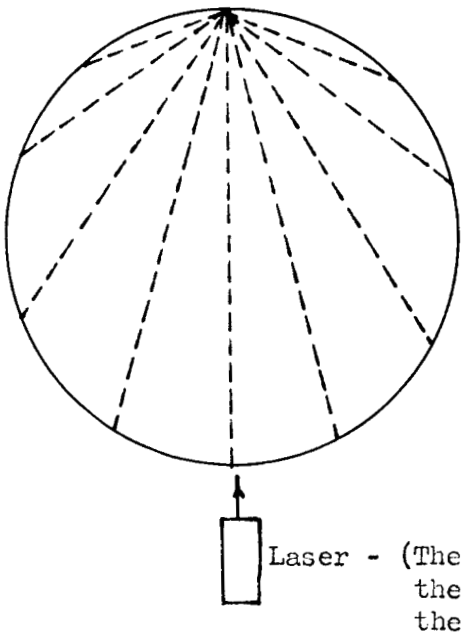

Figure 12

Side view of the sphere on which is plotted the apparent orientations of the plane of polarization of the laser beam reflected from a mirror at the center of the sphere (First order effect only)

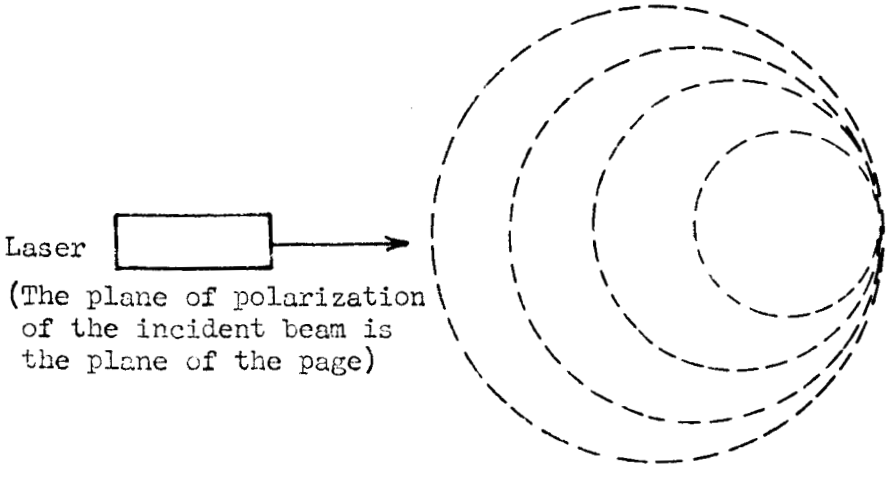

Figure 13

THE USE OF AN ANISOTROPIC PLATE

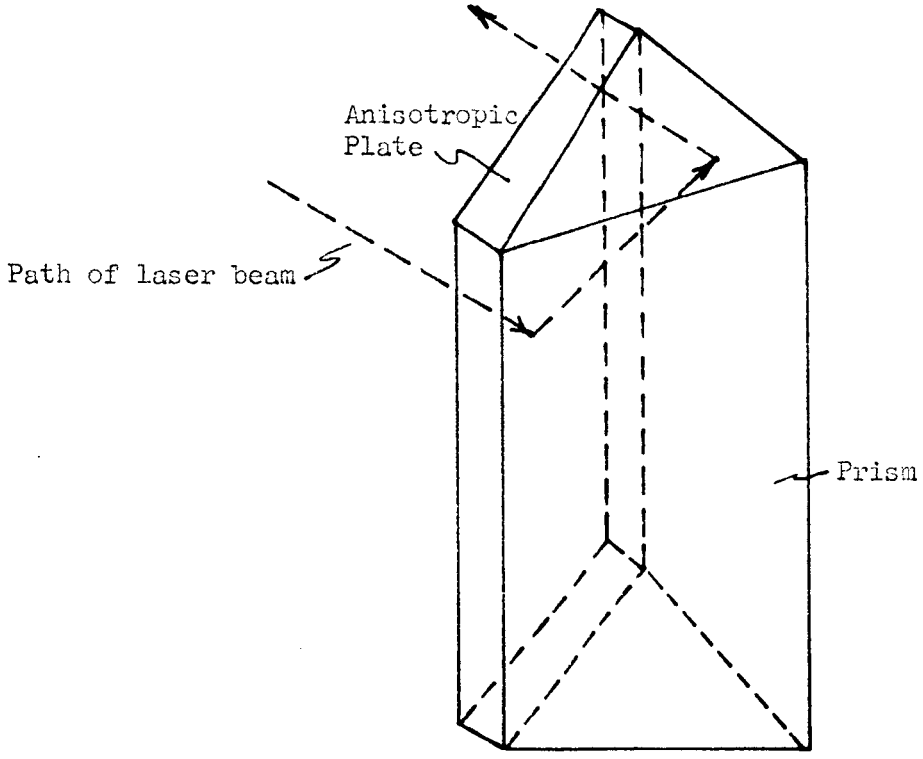

Figure 14

ALTERNATE METHOD OF PHASE COMPENSATION

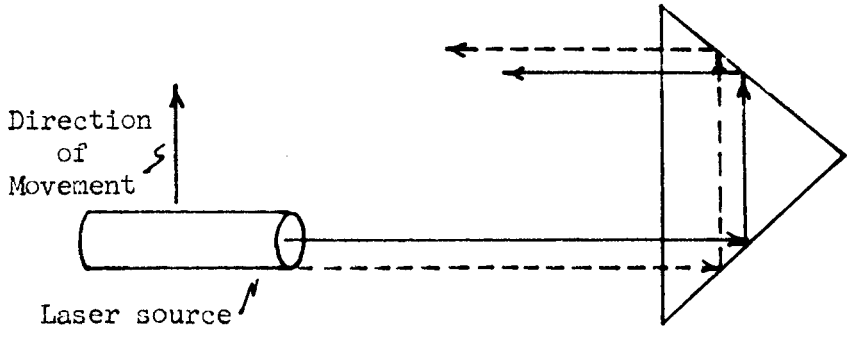

Figure 15

ANGULAR ALIGNMENT DEVICE

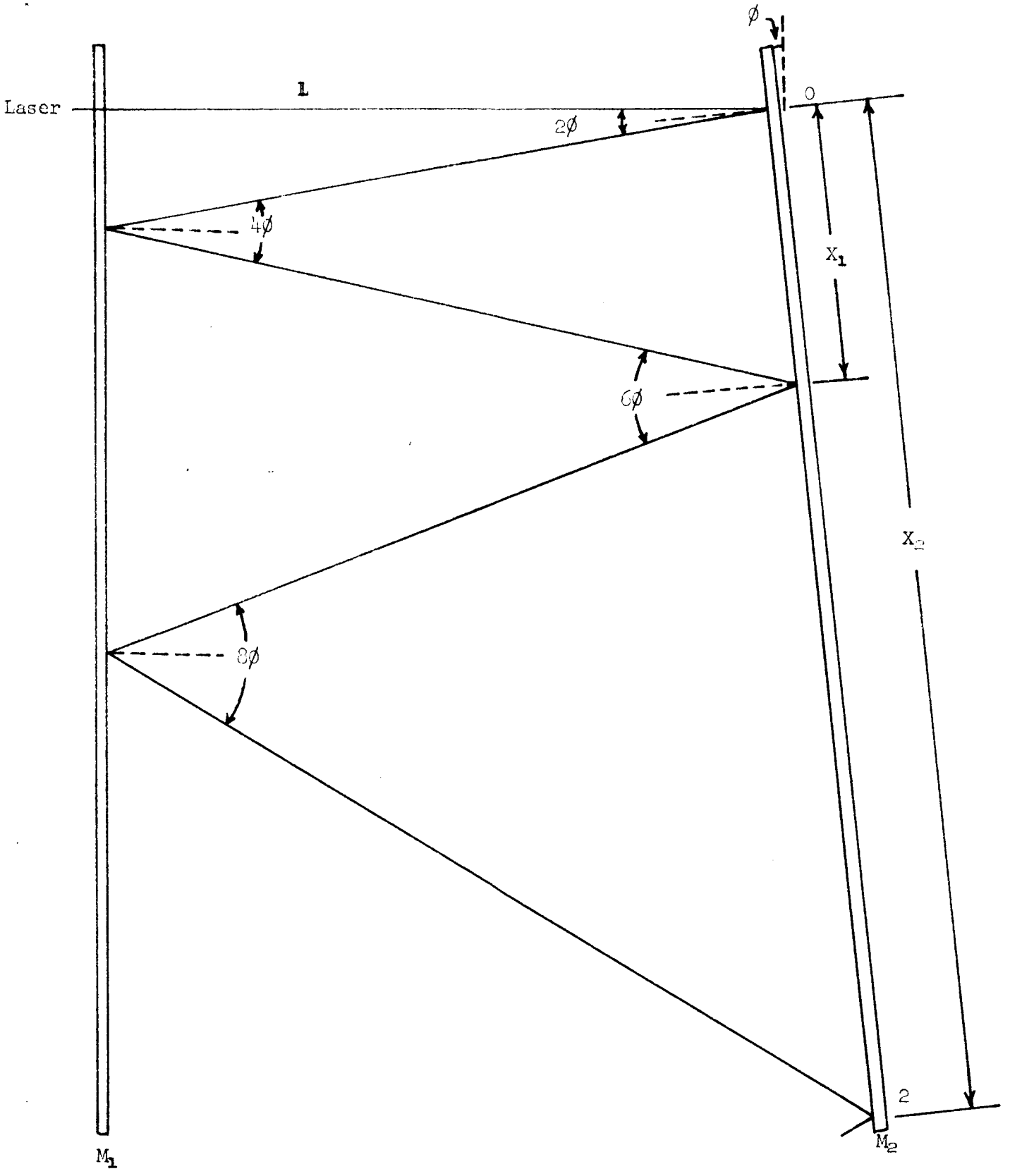

Figure 16

FIRST EXPERIMENTAL ARRANGEMENT FOR RECORDING A HOLOGRAM

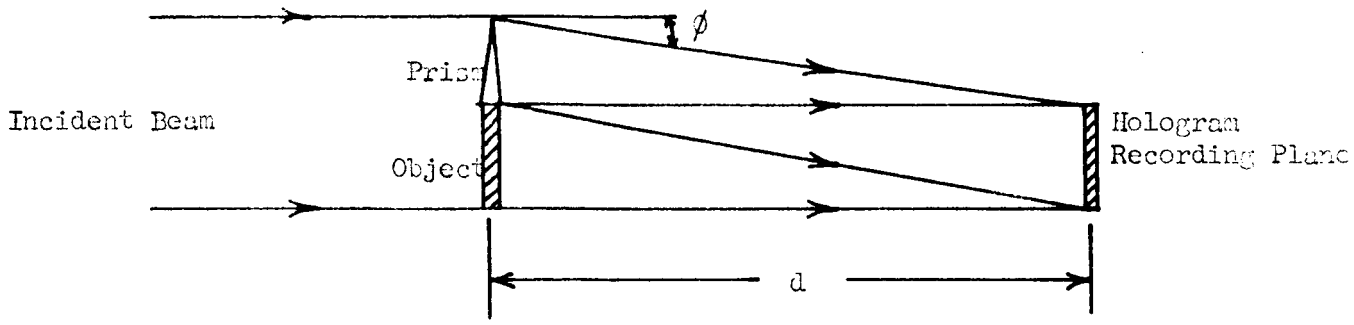

Figure 17

METHOD FOR CONSTRUCTING AN IMAGE FROM THE HOLOGRAM

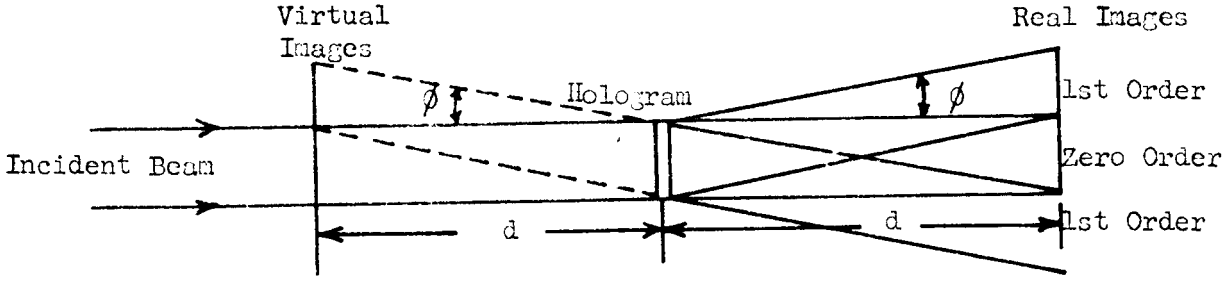

Figure 18

SECOND ARRANGEMENT FOR RECORDING A HOLOGRAM

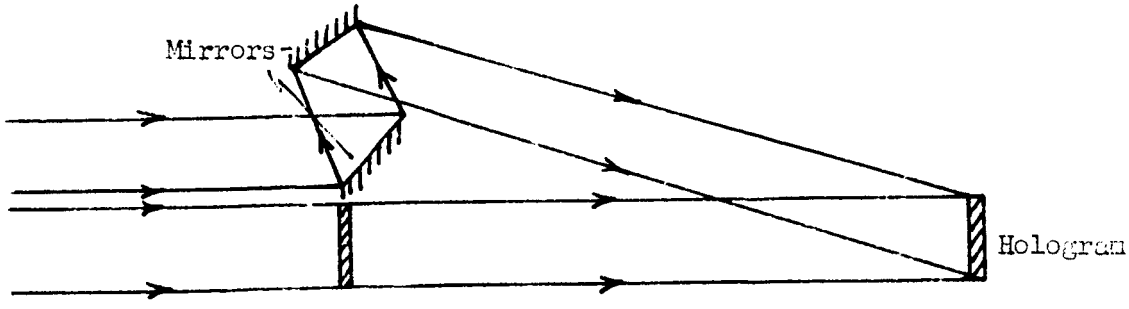

Figure 19

THIRD ARRANGEMENT FOR RECORDING A HOLOGRAM

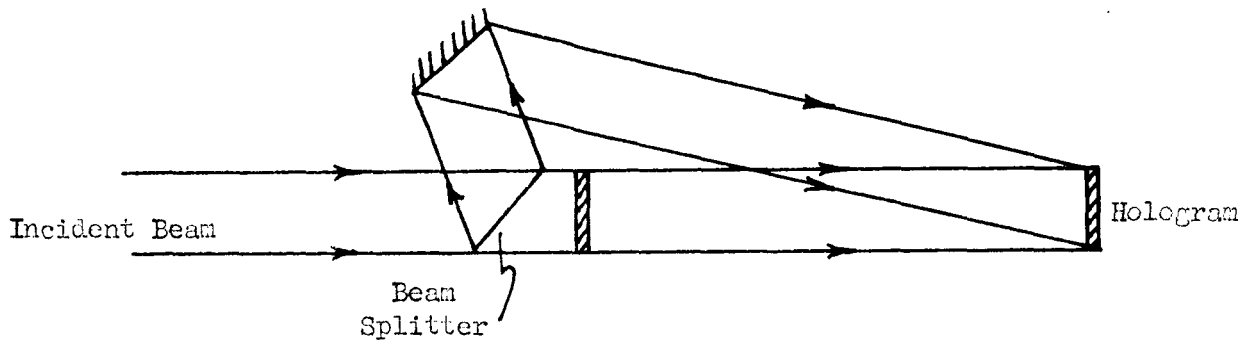

Figure 20

FOURTH ARRANGEMENT FOR RECORDING A HOLOGRAM

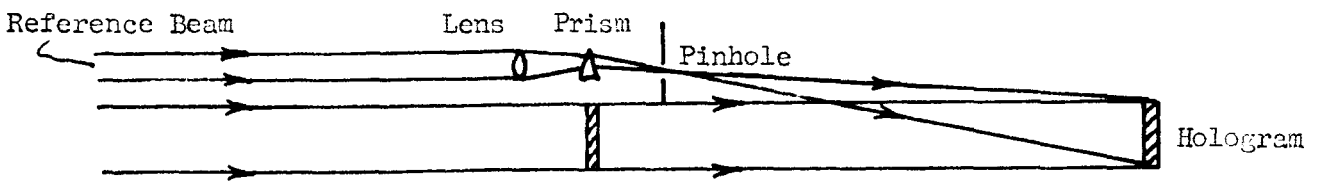

Figure 21a

BEAM OF LIGHT INCIDENT ON AN ASSEMBLY OF PARTICLES

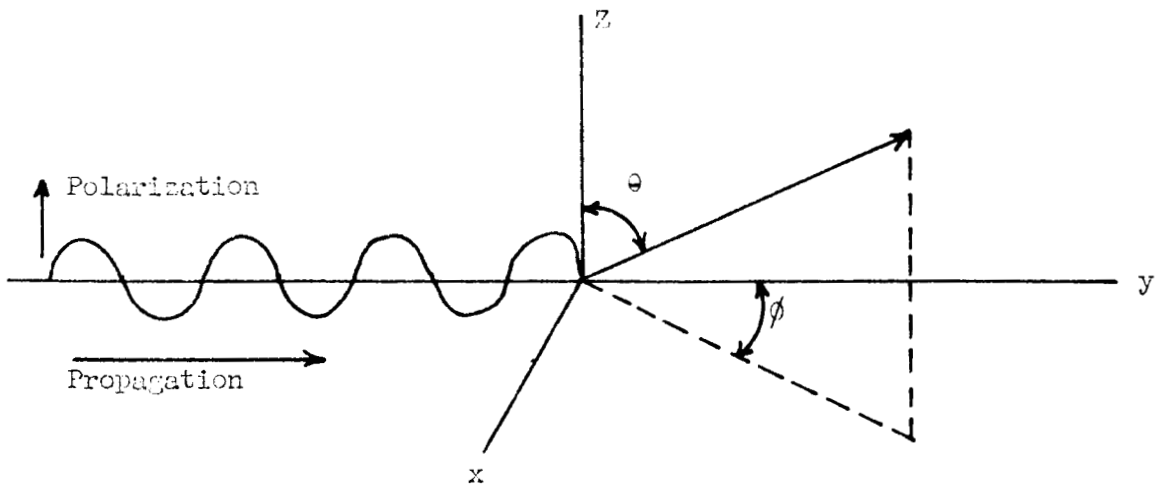

Figure 21b

Figure 21c

LINES OF CONSTANT INTENSITY

Viewed From Above

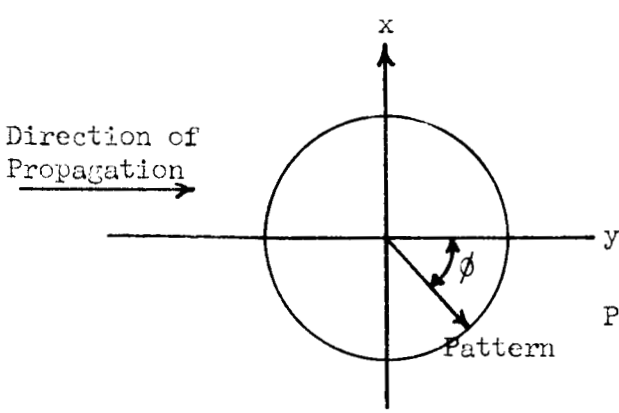

$P = P_Z$; $P_x = P_y = 0$

Viewed From the Side

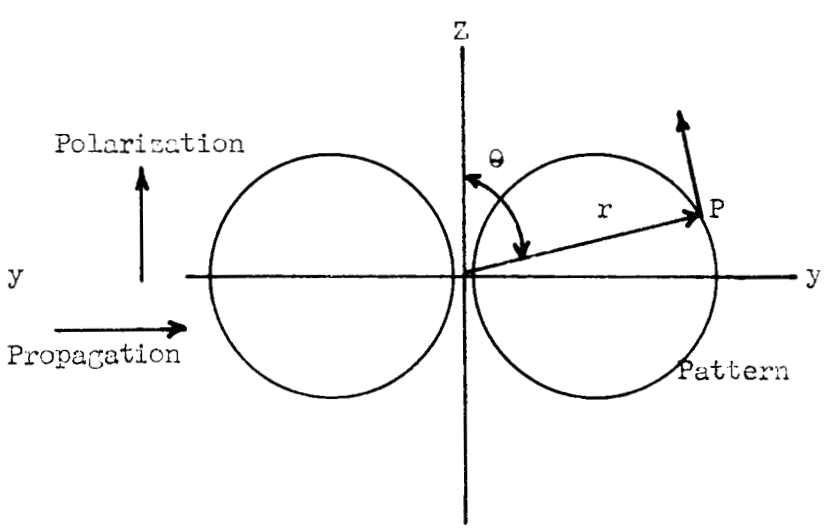

Figure 22a

LIGHT PIPE

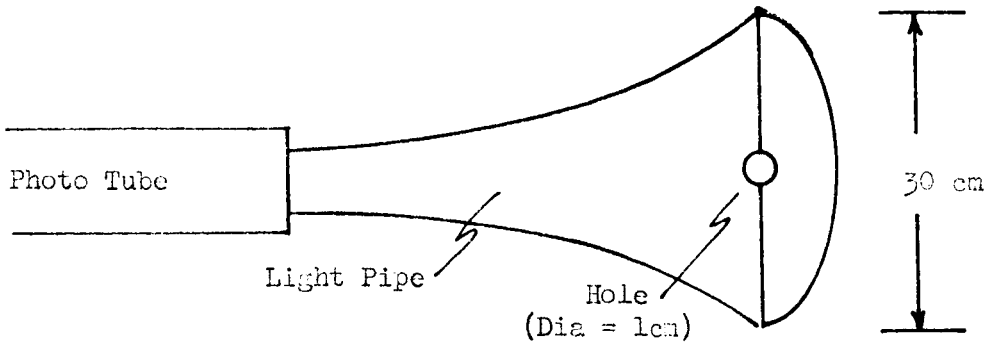

Figure 22b

INTEGRATION SET UP

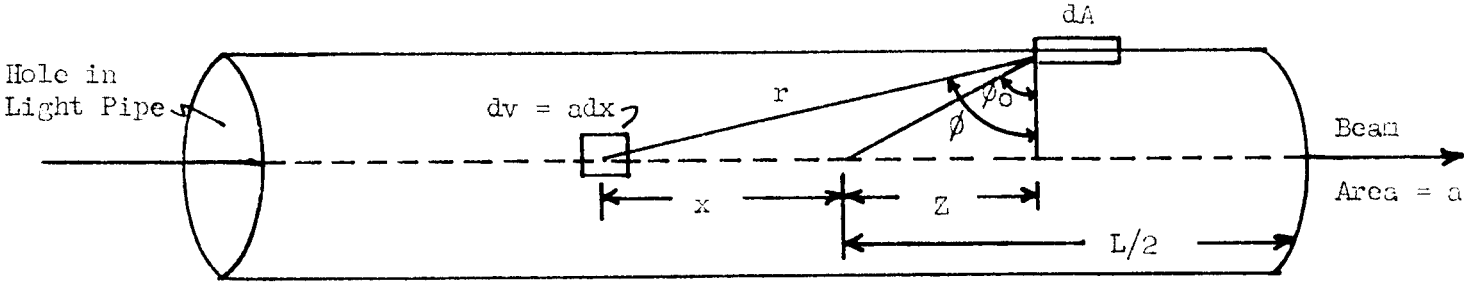

Figure 23

FUNCTION SHAPE

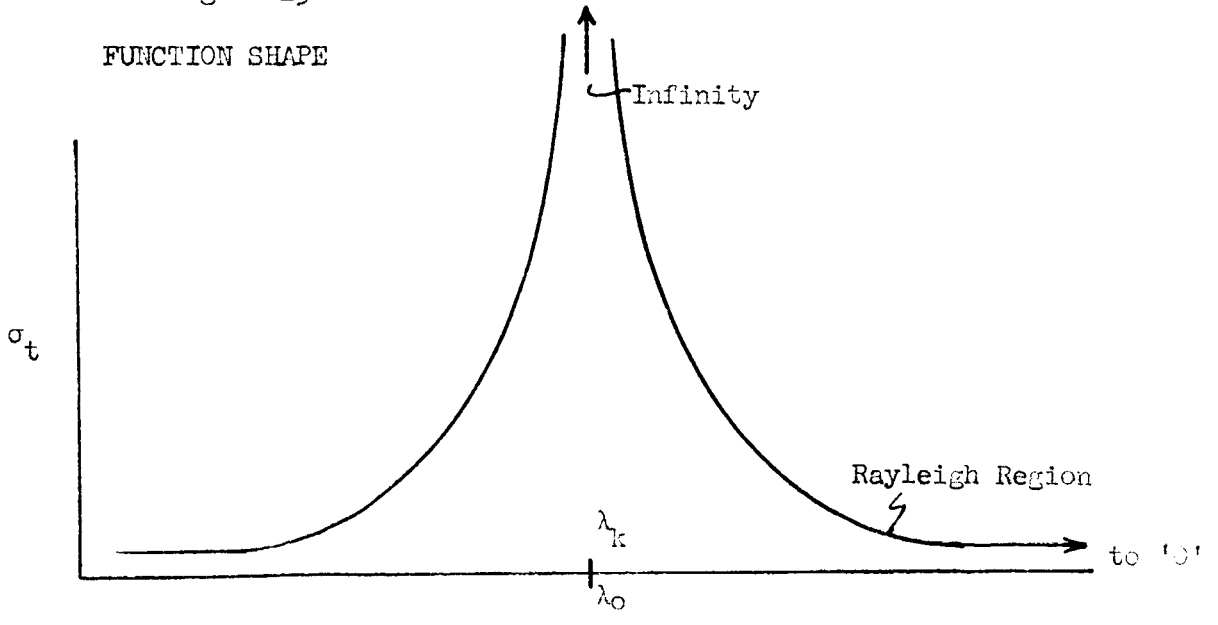

Figure 24

EXPERIMENTAL SET UP FOR MOMENTUM DETECTOR

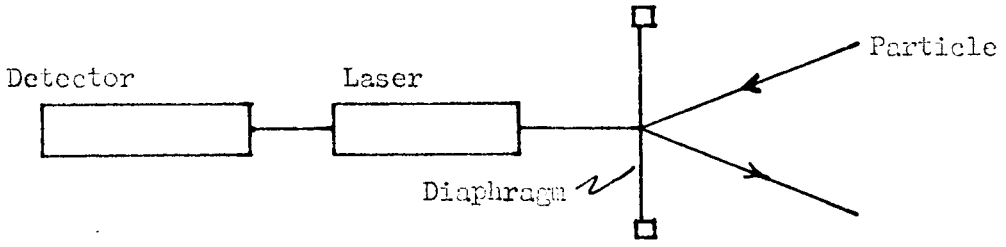

Figure 25

EXPERIMENTAL SET UP FOR OPTICAL DELAY LINE

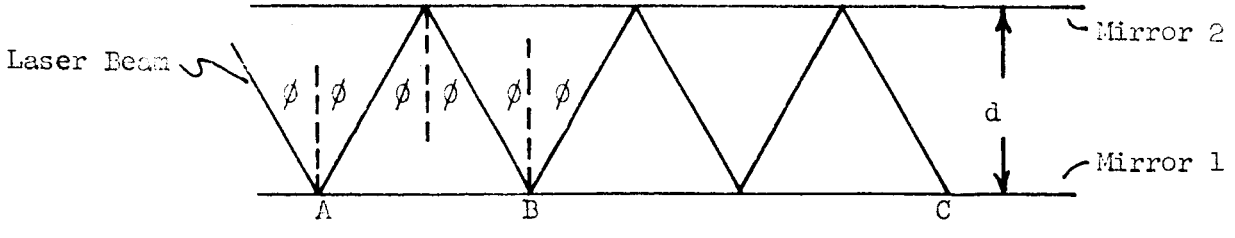

Figure 26

FUNCTIONAL BLOCK APPARATUS

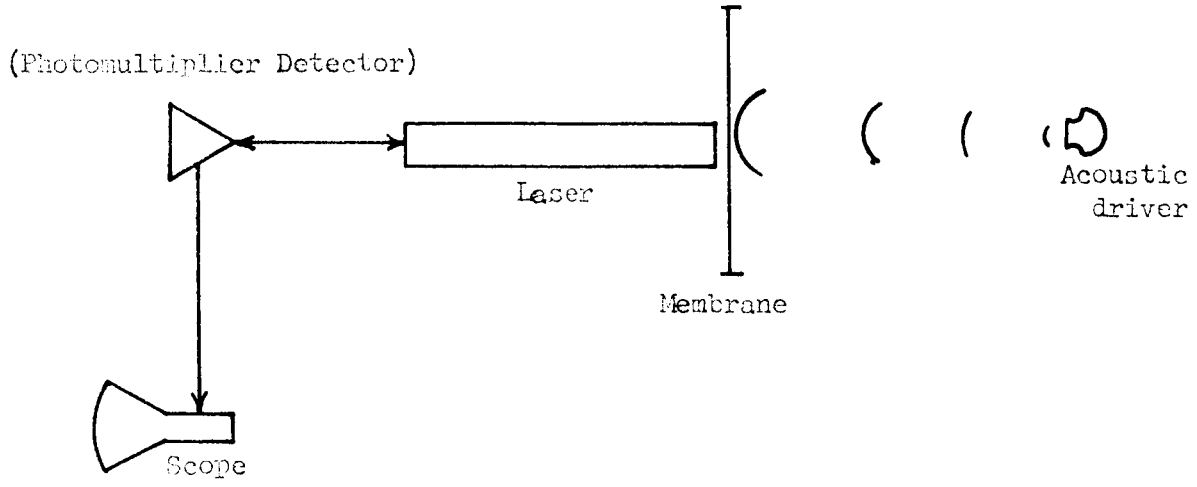

Figure 27

DATA DISPLAY - OSCILLOSCOPE - DOPPLER EFFECT

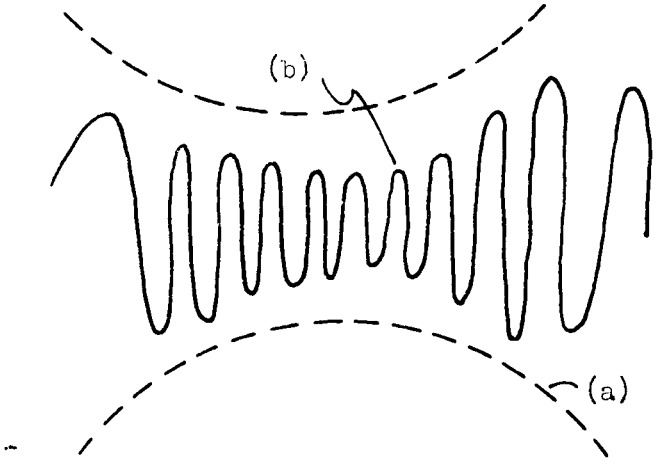

(a) - Shape of curve probably due to reduce quantum on photomultiplier (Further investigation pending)

(b) - Maximum membrane velocity indicated by maximum number of patterns